

Hydrocarbon generation modelling in the Permian and Triassic strata of the Polish Basin: implications for hydrocarbon potential assessment

Dariusz BOTOR^{1, *}

¹ AGH University of Science and Technology, Faculty of Geology, Geophysics and Environmental Protection, al. Mickiewicza 30, Kraków 30-059, Poland; ORCID: 0000-0003-0157-4885



Botor, D., 2023. Hydrocarbon generation modelling in the Permian and Triassic strata of the Polish Basin: implications for hydrocarbon potential assessment. *Geological Quarterly*, 67: 20, doi: 10.7306/gq.1690

Hydrocarbon generation in the Zechstein Main Dolomite and Upper Triassic potential source rocks of the Polish Basin was investigated by 1-D thermal maturity modelling in 90 boreholes across the basin. This identified major zones potentially worthy of further exploration efforts. The maximum burial depth of the Zechstein Main Dolomite and Upper Triassic reached >5 km during the Late Cretaceous leading to maximum thermal maturity of organic matter. Hydrocarbon generation development reveals considerable differences between particular zones of the Zechstein Main Dolomite and Upper Triassic. The kerogen transformation ratio (*TR*) in the Zechstein Main Dolomite reached values approaching 100% along the basin axis. The *TR* in the Upper Triassic source rocks is generally lower than in the Zechstein Main Dolomite due to lesser burial. The Upper Triassic source rocks have the highest *TR* values (>50%) along the basin axis, in the area between boreholes Piła IG 1 and Piotrków Trybunalski IG 1, with the most pronounced zone in the Krośniewice Trough (i.e., between the Krośniewice IG 1 and Budziszewice IG 1 boreholes), where the *TR* reached >90%. The Zechstein Main Dolomite and Upper Triassic entered the oil window in the Late Triassic to Early–Middle Jurassic, respectively. Hydrocarbon generation continued until the Late Cretaceous, and was completed during tectonic inversion of the basin.

Key words: hydrocarbon potential, kerogen transformation ratio, thermal maturity modelling, Polish Basin, Permian, Triassic.

INTRODUCTION

Although petroleum and natural gas exploration in northern Europe has reached an advanced stage, certain stratigraphic intervals are still under-explored (Doornenbal and Stevenson, 2010; Doornenbal et al., 2019). In particular, the Zechstein and Mesozoic strata in the area of the Southern Permian Basin (SPB), extending from the UK to Poland (Van Wees et al., 2000; Maystrenko et al., 2008; Doornenbal and Stevenson, 2010), continues to provide new insights into the geological history of this area, where most hydrocarbon fields are related to the Cambrian to Rotliegend strata (Kilhams et al., 2018a; Underhill and Richardson, 2022). Mesozoic conventional hydrocarbon reserves (>90%) within the SPB are predominantly found in the Netherlands, Germany and Denmark, with only minor amounts associated with the UK and other countries such as Poland (Kus et al., 2005; Pletsch et al., 2010; Kilhams et al., 2018a). This geographical pattern is due to the geological evolution of the SPB area. In particular, the extent of rift systems (e.g., the Central Graben and associated Jurassic source rocks present in a limited area), as well as tectonic inversion, source-rock presence and charge timing influenced on the occurrence of oil and gas fields (Cornford, 1998; Pletsch et al.,

2010; Petersen and Hertle, 2018; Schovsbo and Jakobsen, 2019; Underhill and Richardson, 2022). However, further hydrocarbon discoveries in the Mesozoic strata, for example, in the Polish Basin and other less explored basins are still possible (e.g., Krzywiec et al., 2017a; Kilhams et al., 2018b; Kortekaas et al., 2018). The Zechstein plays on the flanks of the SPB are complex and highly variable. The sedimentary sequence includes repeating evaporite sequences with significant lateral facies variations. Among these there are several dolomite horizons, among which the Zechstein Main Dolomite is still an attractive target with excellent reservoir properties, particularly in areas of platform facies (Peryt et al., 2010; Pletsch et al., 2010; Słowakiewicz and Mikołajewski, 2011; Kosakowski and Krajewski, 2014, 2015; Słowakiewicz et al., 2018; Mikołajewski et al., 2019). Although in the Polish Basin area hydrocarbon deposits also occur in rocks ranging in age from the Cambrian to Permian (Karnkowski, 1999a, b, 2007a, b), recent studies (Kosakowski et al., 2015; Więclaw, 2016; Zakrzewski et al., 2020, 2022a, b) show also that several petroleum source rock horizons exist in the Mesozoic, particularly within Jurassic strata. These studies shed new light into hydrocarbon potential, as summarized by Bachleda-Curuś and Semyrka (1990) and Bachleda-Curuś et al. (1996).

Petroleum exploration in the Mesozoic deposits of the Polish Basin was mainly developed in the years 1947–1970 (Karnkowski, 1996). At that time, the Cretaceous basins with their Jurassic substrate were clearly recognized (Marek and Znosko, 1972). However, positive results in the form of discovered hydrocarbon deposits in Jurassic and Cretaceous reser-

* E-mail: botor@agh.edu.pl

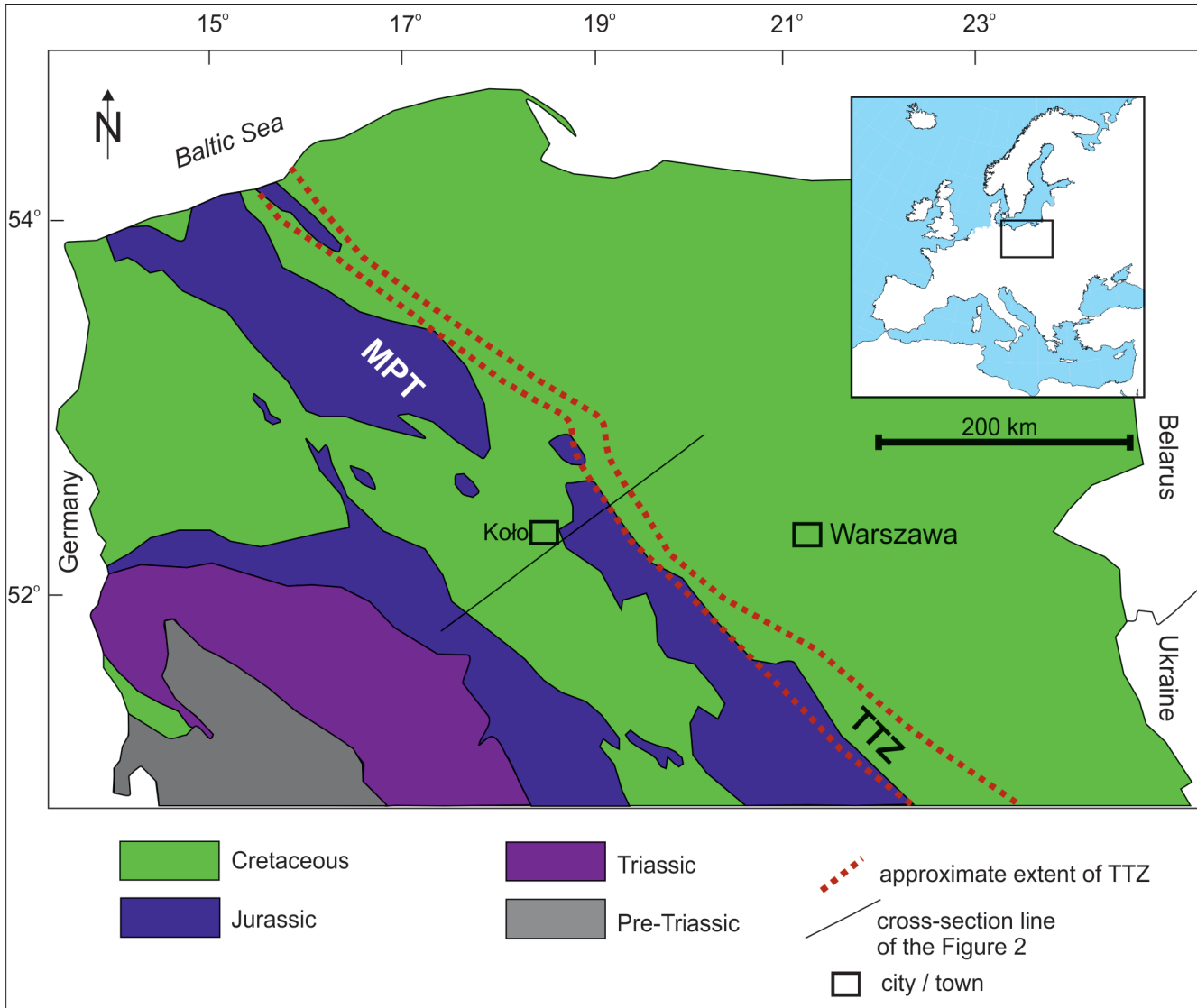


Fig. 1. Simplified sub-Cenozoic map of the Polish Basin (modified after Dadlez et al., 1995, 1998) and location of the study area

TTZ – Teisseyre-Tornquist Zone, MPT – Mid-Polish Trough

voirs were obtained only in the southern extension of the Miechów Trough hidden beneath Miocene strata and the Outer Carpathians. These oil and gas fields may be charged by Paleozoic source rocks (Kotarba et al., 2017a) or the Menilite Shales of Outer Carpathians (Nemčok and Henk, 2006; Botor, 2021). Towards the south, in the Czech Republic Jurassic source rocks (Mikulov Marls) are also recognized (Geršlová et al., 2015). In the central part of the Polish Basin, Middle and Upper Jurassic strata in particular are known to have organic-rich intervals, which contain on average ~1–7% of organic matter of varied thermal maturity (Wilczek, 1986; Kosakowski et al., 2015; Więclaw, 2016; Zakrzewski et al., 2020, 2022a, b). The oil shows found in several boreholes in this area (Mogilno 21, Koło 3 and 4, Dobrów IG 1 and Przybyłów 1 boreholes) are evidence of the possibility of generating and hydrocarbons occurrence in some zones of the Mesozoic strata of the Polish Basin (Karnkowski, 1996).

This study aims to complement previous studies of Paleozoic (Ediacaran up to Rotliegend) petroleum systems in the Polish Basin and adjacent areas, summarized by Kosakowski et al. (2010), Botor et al. (2013, 2019a, b), and Papiernik et al.

(2019), and to provide a new detailed regional overview of the burial and maturation history of important stratigraphic intervals of the Polish Basin. In this paper, one-dimensional (1-D) hydrocarbon generation modeling of the (i) Zechstein Main Dolomite and (ii) Upper Triassic potential source rocks was performed, which allowed construction of regional maps of the development of organic matter maturity and kerogen transformation ratio into hydrocarbons across the Polish Basin. Jurassic source rocks were discussed recently by Kosakowski et al. (2015), Więclaw (2016) and Zakrzewski et al. (2020, 2022a, b).

GEOLOGICAL SETTING

The Polish Basin (Fig. 1), together with its axial, most deeply subsiding part called the Mid-Polish Trough (MPT), is part of the Permian and Mesozoic epicontinental basins of Western and Central Europe, sometimes called the Central European Basin System (e.g., Scheck-Wenderoth et al., 2008). Here the geological history of the studied area is briefly outlined, focusing on the aspects particularly relevant to the present modelling study.

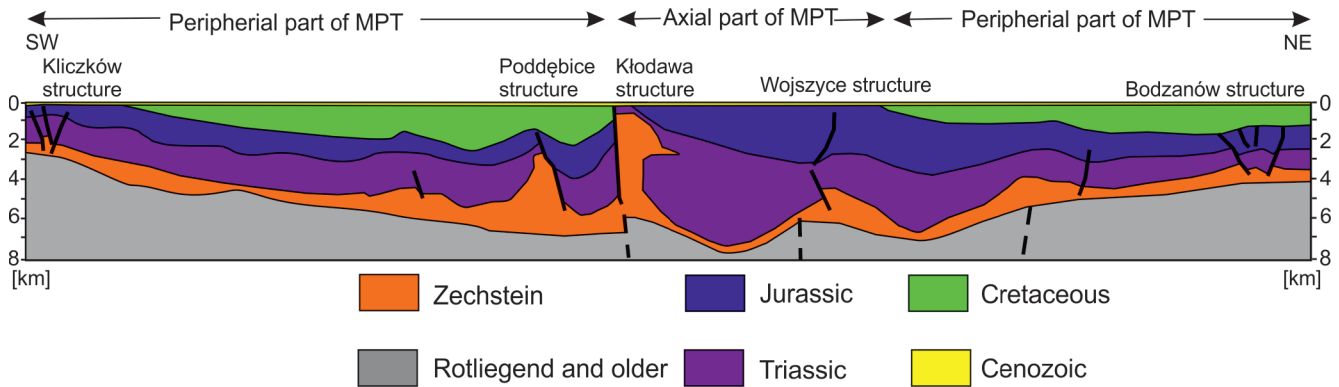


Fig. 2. Cross-section through the central part of the Polish Basin (modified after Krzywiec, 2004; Scheck-Wenderoth et al., 2008; Krzywiec et al., 2017a)

The MPT developed along the Teisseyre-Tornquist Zone (TTZ; Kutek and Głazek, 1972; Pożaryski and Brochwicz-Lewiński, 1978; Dadlez et al., 1995; Kutek, 2001; Mazur et al., 2021), one of the key tectonic lineaments in Europe located at the transition between the East European Precambrian Craton and the West European Paleozoic Platform (see Mazur et al., 2021 for recent summary and further references). The substrate of the Polish Basin includes a sedimentary cover, a few kilometres thick, of Ediacaran to Carboniferous strata. The Polish Basin consists of the extensive Permian-Mesozoic succession, which is unconformably overlain by up to 350 m of Cenozoic strata (Piwocki, 2004; Fig. 2). The Permian to Cenozoic succession reaches ~8 km in total thickness along a NW–SE-oriented depocentre in the MPT (e.g., Dadlez et al., 1995; Scheck-Wenderoth and Lamarche, 2005; Mazur et al., 2005, 2021). The Permian to Mesozoic of the Polish Basin displays a sedimentary succession reflecting continental to open-shelf depositional systems (Marek and Pajchłowa, 1997; Figs. 3 and 4). Towards the flanks, it thins to 2–5 km. The sedimentary succession includes several erosional surfaces, of which the most important formed in the Early Jurassic and Early Cretaceous (Marek and Pajchłowa, 1997). Depocentre locations of particular stratigraphic units shifted through time but were mostly limited to the MPT area. The Polish Basin subsidence is related to crustal extension followed by lithospheric cooling. Structural orientation was strongly dependent on the pre-existence of the structure of the TTZ (Mazur et al., 2021). A rifting phase occurred during the Permian–Early Triassic, and an accelerated subsidence phase took place during the Late Jurassic, linked to rifting of the North Atlantic system and to the Tethyan margin. Subsidence accelerated at the beginning of the Cenomanian and marks the beginning of compressive deformation, which culminated with basin inversion at the end of the Cretaceous (Dadlez et al., 1995; Stephenson et al., 2003; Krzywiec et al., 2018). Evolution of the MPT was strongly influenced by Zechstein salt movements from the Early Triassic, and continued throughout the entire Mesozoic (e.g., Rowan and Krzywiec, 2014). This led to the complex system of salt structures in the central and NW parts of the MPT (for details see Krzywiec, 2004, 2006a, b). In the axial part of the MPT, Late Cretaceous open marine sedimentation was terminated by Late Cretaceous/Early Paleogene tectonic inversion leading to significant erosion. The sedimentary deposits were removed down to the Lower Jurassic or even Upper Triassic along the axis of the MPT and in the SW part of the Polish Basin (e.g., Botor et al., 2013). In some areas of the MPT, exhumation began in the latest Turonian–early Campanian and ~2 km of Mesozoic rocks were removed (Resak et al., 2010; Krzywiec et al., 2018; Botor

et al., 2018; Łuszczak et al., 2020). Late Cretaceous tectonic inversion is widely recognized in central Europe and was summarized recently by von Eynatten et al. (2021). A compilation of several hundred published thermochronological analyses (apatite fission-track analyses and apatite helium dating) indicates generalized, km-scale exhumation over substantial parts of Central Europe in Late Cretaceous to Paleocene time. Tectonic inversion was caused by a combination of (i) collisional phases in the Alpine and Carpathian orogens and (ii) development of the Atlantic (Ziegler, 1990a, b; Dadlez et al., 1995; Mazur et al., 2005). The Permian to Mesozoic evolution of the Polish Basin was summarized and reviewed by Dadlez et al. (1995), Krzywiec (2002, 2006a, b, 2009), Lamarche et al. (2003), Mazur et al. (2005) and Dadlez (2006).

OVERVIEW OF THE PETROLEUM SYSTEM ELEMENTS IN THE STUDY AREA

CARBONIFEROUS–PERMIAN (ROTLIEGEND)

In the Polish Basin, numerous natural gas fields occur in Permian (Rotliegend) strata (Karnkowski, 1999a,b, 2007a, b). Gas is accumulated mainly in aeolian sandstones and, subordinately, in fluvial sandstones (Pletsch et al., 2010; Kiersnowski, 2013). Additionally, in Western Pomerania, Carboniferous (Namurian) fluvial sandstone reservoirs also exist. Gas fields are associated with both conventional traps and unconventional accumulations (tight sand; Kiersnowski et al., 2010). The source rocks for the Rotliegend gas fields are Carboniferous strata that consist mainly of Lower Carboniferous claystones and mudstones with dispersed organic matter (usually <2% total organic carbon; TOC) that were deposited in the Variscan foreland basin (Kotarba et al., 2005; Botor et al., 2013). These source rocks contain kerogen mostly of gas-prone Type III; however, subordinately, kerogen of algal marine origin and mixed Type II/III occur also. The kerogen thermal maturity progressively increased with depth, from ~0.5% mean random vitrinite reflectance (VR) in marginal parts of the Carboniferous basin to >5.0% VR at the bottom of the Lower Carboniferous (Pletsch et al., 2010; Botor et al., 2013).

In the Carboniferous source rocks, hydrocarbon generation began in rapidly subsiding areas (Pletsch et al., 2010; Botor et al., 2013) in the Late Carboniferous. These processes were halted by Variscan tectonic inversion at the end of the Carboniferous. However, hydrocarbon generation resumed in Mid-Triassic to Late Jurassic and in Late Cretaceous times. The main migration event took place during the Triassic to Jurassic, while the Late Cretaceous migration phase was less intense (Pletsch

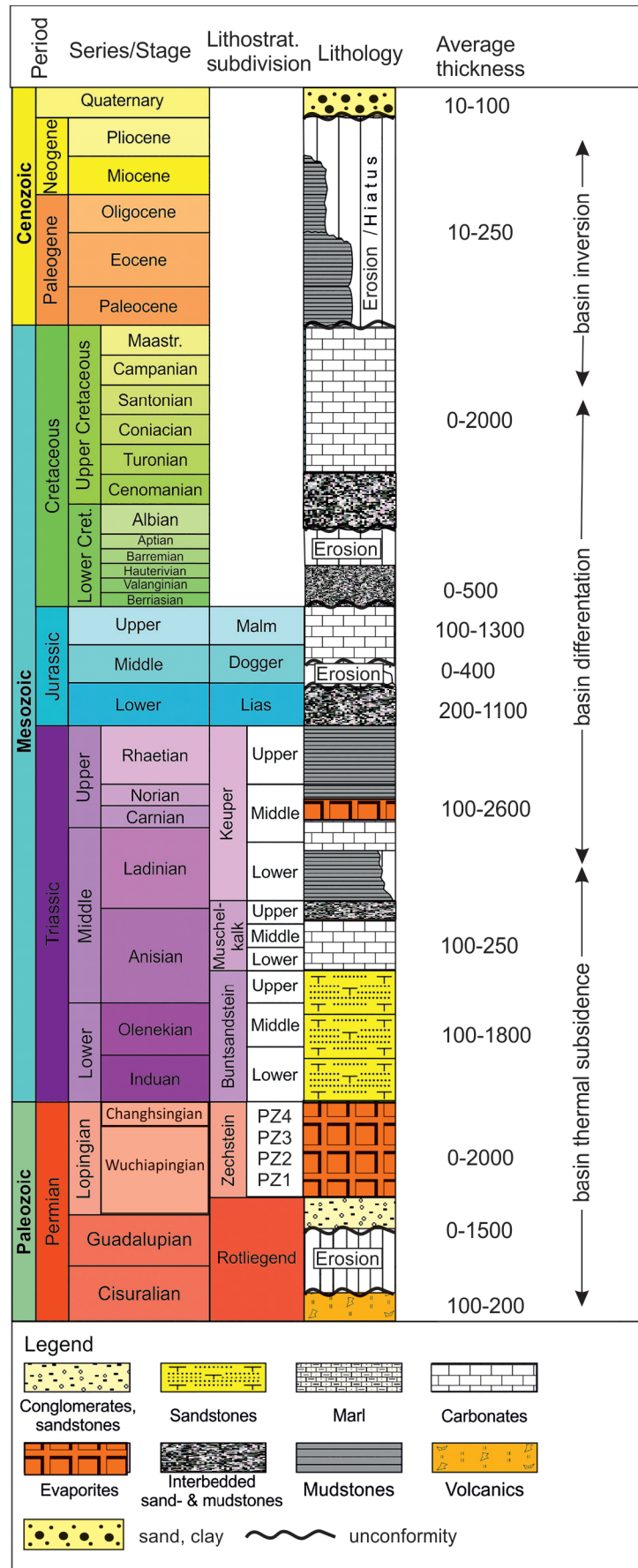


Fig. 3. Simplified lithostratigraphic chart showing the dominant lithology and thickness of the Permian to Cenozoic strata of the Polish Basin (modified after Marek and Pajchłowa, 1997; Dadlez et al., 1998)

The sedimentary succession is punctuated by several erosional and/or hiatus episodes, of which the most important are the Rotliegend, Early–Middle Jurassic, Early Cretaceous and Paleogene–Neogene

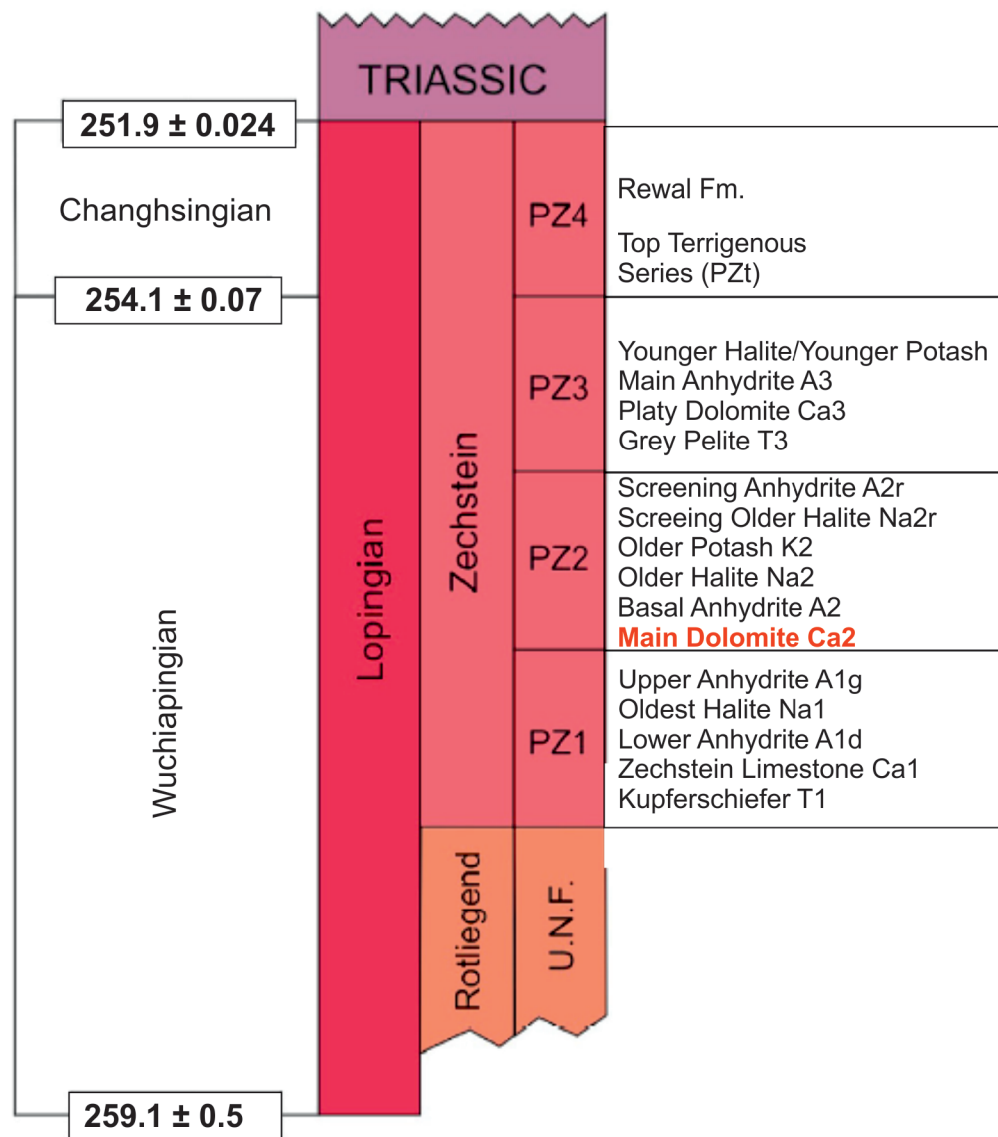


Fig. 4. Stratigraphy of the Zechstein in the Polish Basin modified after Wagner (1994, 2001)

Zechstein stratigraphic boundaries after Peryt and Peryt (2021); correlation of the Zechstein and the Wuchiapingian/Changhsingian boundary after Szurlies (2020); U.N.F. – Upper Noteć Formation

et al., 2010; Botor et al., 2013). Rotliegend hydrocarbon traps were formed as mainly structural or geomorphological features (Kiersnowski and Tomaszczyk, 2010). The natural gas content varies by region. Generally, the eastern gas fields have high a methane content (up to >80%), with the western fields having a low methane content and a high nitrogen content. In the deeper part of the Rotliegend Basin, significant porosity reduction and rapid reduction of sandstone permeability are observed; however, tight gas fields were discovered (Kiersnowski et al., 2010).

ZECHSTEIN MAIN DOLOMITE

The Zechstein Main Dolomite petroleum system is unique in that the carbonates and evaporites of a Zechstein (PZ2) single depositional cycle (Wagner, 1994; Peryt et al., 2010) constitute the petroleum source rocks, the reservoir rocks and the regional top seals (Kotarba and Wagner, 2007; Pletsch et al., 2010;

Słowakiewicz and Mikołajewski, 2011; Kosakowski and Krajewski, 2014, 2015; Kotarba et al., 2017b, 2020; Krzywiec et al., 2017a; Słowakiewicz et al., 2018; Mikołajewski et al., 2019). More than 90 petroleum deposits have been discovered in the Zechstein Main Dolomite reservoir in Poland (Karnkowski, 1999a, 2007a, b). The salts and/or anhydrite are widely thought to be a top seal of this petroleum system. The depth of hydrocarbon migration into the evaporites is estimated at several tens of metres in the case of undisturbed salt strata (Kovalevych et al., 2008). However, hydrocarbon migration can involve longer distances in the case of salt diapirs (e.g., Toboła and Botor, 2020). The major Zechstein Main Dolomite source rocks are the laminated carbonate mudstones and boundstones deposited in low-energy lagoons on the marginal Zechstein Main Dolomite platform or on isolated platforms, that locally contain an abundant amount of organic matter (>20 wt.% TOC; Słowakiewicz and Mikołajewski, 2011). Petroleum in the Zechstein Main Dolomite was mainly generated

from microbial-algal organic matter types I and II (Kotarba and Wagner, 2007; Słowakiewicz and Mikołajewski, 2011; Kosakowski and Krajewski, 2014, 2015; Słowakiewicz et al., 2018; Mikołajewski et al., 2019; Kotarba et al., 2020). Very good reservoir rocks occur close to the source rocks; however, reservoir properties are highly variable, both laterally and vertically (Pletsch et al., 2010; Słowakiewicz and Mikołajewski, 2011; Kosakowski and Krajewski, 2014, 2015; Słowakiewicz et al., 2018; Mikołajewski et al., 2019).

TRIASSIC

In the Triassic Period, the Polish Basin was located at the northern periphery of the Western Tethys Ocean, in which sedimentation was strongly influenced by inherited Variscan structures which controlled the basin differentiation and subsidence pattern (Szulc, 2007). However, the MPT was the main depocentre. Upper Triassic sedimentary sequences are characterized by a predominance of clastic, mainly terrestrial deposits (Szulc, 2007). Dry climatic conditions dominated during the Late Triassic, but several humid intervals have also been recognized during this time in the central European area (Reinhardt and Ricken, 2000). Upper Triassic strata are dominantly fluvial and lacustrine, locally comprising organic-rich clastic deposits, including thin coal seams (Szulc, 2000). Non-marine, lacustrine environments are widely known as very good source rocks in many parts of the world (e.g., see summary in Katz and Lin, 2014). Lacustrine sequences are increasingly being recognised as hosts for commercial hydrocarbon reserves. Various types of organic matter in lacustrine sequences have organic carbon contents in the range ~1–20% (Powell, 1986; Bohacs et al., 2000; Petersen et al., 2004; Katz and Lin, 2014; Behar et al., 2020; Do Couto et al., 2021).

In the Polish Basin, no hydrocarbon accumulations have been found in Triassic rocks so far. However, reservoir rocks are present in the Lower Triassic of Central Europe, though the nature of the petroleum charge and seal are uncertain (Bachmann et al., 2010; Pletsch et al., 2010). In the Polish Basin, the porosity of Lower Triassic rocks is in the range 3–12% (Sowizdżał et al., 2013). The source rock potential of Triassic strata has not yet been fully constrained by geochemically. Exploration for further Triassic-hosted oil and gas could continue across the basin, especially in relatively underexplored areas where data can be reinterpreted in the context of new research (e.g., Krzywiec et al., 2017a). Therefore, detailed identification of source rocks would allow for better assessment of the petroleum system. So far, in the Rhaetian of offshore Denmark, NW Germany and the Netherlands, thin coal intervals provide a local hydrocarbon source (Nielsen, 2003; Geluk et al., 2018), that suggests the presence of such horizons also towards the east in the Polish Basin. In Denmark, Triassic strata are dominated by continental to marginal marine sandstones, mudstones, carbonates and evaporites, and good quality source rocks are not common. Apart from a few local occurrences of Upper Triassic units with limited potential (e.g., the 73 m-thick mudstone-dominated Gassum Formation), the Triassic does not possess petroleum generation potential (Petersen et al., 2008). In the Triassic succession of Germany, black claystones and coals are suggested to have minor gas generation potential and are regarded as a possible source of gas shows in a number of boreholes penetrating Lower Triassic rocks (Lutz and Cleintuar, 1999). In the Middle Triassic, partly bituminous marls, limestones and dolomites ~10 m thick have also been described (Eisbacher and Fielitz, 2010). In the Upper Triassic (Keuper – i.e. lower part of the Upper Triassic), only the Lettenkeuper Member is assumed to have minor gas generation potential

due to interbedded thin coal layers. These layers are described as partly bituminous (Schad, 1962). In the Upper Triassic, locally enrichment in TOC was observed in the range ~1–3 % (Schobben et al., 2019).

Generally, in the Upper Triassic of the Polish Basin, few geochemical investigations are available indicating mild hydrocarbon generation potential with TOC values of typically ~1–2%, of mixed II/III type kerogen (Bachleda-Curuś and Semyrka, 1990; Bachleda-Curuś et al., 1996; Marynowski et al., 2006; Marynowski and Simoneit, 2009; Wójcicki et al., 2022). In the Rhaetian strata, TOC is usually below 1%, except for some lacustrine mudstones, where TOC content can reach 4% (Pieńkowski et al., 2020). In many boreholes Upper and Middle Triassic TOC values are up to 0.6%. The thermal maturity of these claystones is in the range of ~0.8–1.1% VR (e.g., Piła IG 1, Objezierze IG 1 boreholes), suggesting that these kerogens achieved the mid-oil window stage (Kiersnowski, 2017; Dyrka, 2017; Żuk, 2019). In the central part of the Polish Basin, the Lower Keuper source rocks have an average thickness of 67 m (based on 66 boreholes), usually ranging from 50 to 100 m (Bachleda-Curuś and Semyrka, 1990). The average TOC is 0.9 wt.% in these rocks. Generation of $1.6 \cdot 10^6$ Mg hydrocarbons per 1 km³ of source rocks was calculated by Bachleda-Curuś and Semyrka (1990) applying the TTI method (Waples, 1980).

JURASSIC

In the Polish Basin, Upper Jurassic source rocks show up to 7.5 wt.% TOC, while Middle Jurassic strata contain up to ~5 wt.% and Lower Jurassic up to ~1.1 wt.% TOC (Wilczek, 1986; Kosakowski et al., 2015; Więclaw, 2016; Zakrzewski et al., 2020, 2022a, b). Geochemical data indicate the presence of mixed organic matter (kerogen type III/II) occurring in the Upper Jurassic, whereas gas-prone type III kerogen prevails in the Middle and Lower Jurassic. However, type IV kerogen also constitutes a significant part of the organic matter (Zakrzewski et al., 2020, 2022a, b). Geochemical data indicate that the Lower Jurassic strata contain partially reworked kerogen, which even just after deposition had poor hydrocarbon potential (Zakrzewski et al., 2022a). In the Lower and Upper Jurassic succession, thermal maturity is in the range of 0.7–0.8% VR in the deeply buried part of the Mogilno-Łódź Synclinorium. In the Lower Cretaceous rocks, the thermal maturity did not exceed 0.5% VR. The thermal maturity of organic matter in these source rocks ranges from the immature phase to the early and mid-phase of the oil window. This is indicated by the results of VR and Rock-Eval temperature Tmax as well as by biomarkers (Kosakowski et al., 2015; Więclaw, 2016; Zakrzewski et al., 2020, 2022a, b). The onset of hydrocarbon generation from the Jurassic source rocks occurred during the Cretaceous, at a burial depth >2.5 km and temperature >80°C. The generation was completed at the end of Cretaceous due to tectonic inversion. The kerogen transformation reached up to ~40% in the Middle Jurassic and up to ~10% in the Upper Jurassic source rocks (Kosakowski et al., 2015).

In the Polish Basin, no oil and gas fields have been discovered in Mesozoic strata. Potential reservoirs might constitute sandstone units of the Lower Triassic, Lower and Middle Jurassic and Cretaceous, as similar to the North Sea area (Pletsch et al., 2010; Tarkowski and Wdowin, 2011; Sowizdżał and Semyrka, 2016). The most promising reservoirs are porous Lower and Middle Jurassic sandstones forming structural and combined structural-stratigraphic traps (Labus et al., 2014; Labus and Tarkowski, 2022). The stratigraphic traps likely exist in the form of bioherms within the Oxfordian limestones, as well

as in Lower Cretaceous sandstones, and channel-filling facies of fluvial sandstones of the Upper Triassic, where natural gas shows have been observed in the Koło area (Wójcik et al., 2022). Potential traps are likely related to salt tectonics and may include anticlinal structures above salt pillows, through structures induced by inversion, and combined structural-stratigraphic traps next to salt diapirs (Krzywiec et al., 2017a; Wójcik et al., 2022). The traps were formed during Late Cretaceous inversion, as well as due to movements of Zechstein evaporites during the entire Mesozoic. Traps were mainly sealed by the shales in the Mesozoic succession and evaporites in the Zechstein (Krzywiec et al., 2017a; Wójcik et al., 2022).

METHODS AND DATA

BASIN MODELLING TECHNIQUE

The 1-D numerical models were constructed with the use of *PetroMod* software (Schlumberger) for 90 boreholes. Numerical modelling techniques enable the simulation of the complex set of interacting physical and chemical processes taking place during the evolution of a sedimentary basin. The quantification of geological evolution is based on a conceptual model, which describes the geological evolution of the study area (Waples et al., 1992; Hantschel and Kauerauf, 2009). The conceptual model was constructed in a temporal framework in which geochronologic entities called 'events' form the basis of the temporal framework and the input data. Input data for each event consist of duration, depositional or erosional thickness, lithology, bathymetry, sediment/water interface or surface temperature, and heat flow. Petrophysical parameters such as porosity, density, thermal conductivity, etc., are then defined from the lithology. After each simulation run, the calculated results have to be compared with measured values, in order to calibrate the model and check its geological reliability. The major calibration parameter was mean random vitrinite reflectance values (*VR*). The kinetic EASY % R_o approach was applied, which enables the calculation of the mean random vitrinite reflectance up to the value of 4.6% (Sweeney and Burnham, 1990; Burnham et al., 2016). Calibration was achieved mainly by varying heat flows or original thicknesses of now eroded sedimentary units within geologically reasonable limits (Wygrala, 1989; Waples et al., 1992; Hantschel and Kauerauf, 2009). Initially, heat flow assignment for the past stages of basin history is estimated based on the tectonic setting (Hantschel and Kauerauf, 2009). Further palaeo-heat flows values are assessed by the modelling procedure in order to achieve the best fit between the calculated model and measured calibration parameters. Heat flow values are best constrained for times of maximum temperature which usually correspond to maximum burial depth (Waples et al., 1992; Hantschel and Kauerauf, 2009). During modelling, different burial-uplift scenarios are tested to find a model, which is best calibrated with *VR* values measured on rock samples. More details on the principles of the modelling technique are given elsewhere in, e.g., Waples et al. (1992) and Hantschel and Kauerauf (2009).

MODELLING INPUT DATA

A set of stratigraphic and lithological data concerning the boreholes studied was based on published data and interpretations concerning the geological evolution of the Permian–Cenozoic in the Polish Basin. Particularly useful were palaeothickness and palaeofacies maps of Permian and Mesozoic sequences as well as regional cross-sections of the study area (Marek and Pajchlowa, 1997; Dadlez, 2006). Basic stratigraphic and

lithological data were compiled from reports provided by the Central Geological Database of the Polish Geological Institute (PGI) in Warsaw: <http://otworywiertnicze.pgi.gov.pl/Details/Information/> and the Polish National Geological Archives <https://www.pgi.gov.pl/en/narodowe-archiwum-geologiczne-2.html>

Periods of sedimentation and erosion/non-deposition, sediment types and thicknesses were identified for each borehole. The age (in Ma) of standard chronostratigraphic units is given after Ogg et al. (2008). Defined PetroMod lithologies (with petrophysical properties determined for each rock type) are given in Table 1 and were defined on the basis of detailed lithological descriptions of core and cutting material included in borehole documentations. Palaeo-heat flow values were selected based on the quality of fit between the model predictions and actual observations of thermal maturity–depth profiles. The present-day heat flow values were interpolated from the surface heat flow maps (Majorowicz and Wybraniec, 2011; Majorowicz, 2021). The values obtained range from 40 to 78 mW/m². Mapping was based on the latest available geothermal data from boreholes across the Polish Basin, carefully verified in order to exclude unreliable measurements. Methodological problems related to heat flow calculation and mapping were thoroughly discussed by Majorowicz and Wybraniec (2011), and Majorowicz (2021). However, present-day heat flow values do not influence the maturation history of inverted basins (as generally in this case), which is governed mainly by a pre-inversion period (Waples et al., 1992; Hantschel and Kauerauf, 2009).

Mean random vitrinite reflectance measurements were implemented in the numerical modelling procedure as major parameters calibrating the burial and thermal history of the basin (e.g., Hantschel and Kauerauf, 2009). Thermal maturity values included several sources of data (Bachleda-Curuś and Semyrka, 1990; Bachleda-Curuś et al., 1996; Grotke 1998, 2006; Wagner, 1999; Kotarba et al., 2005, 2006; Resak et al., 2008) and the Central Geological Database of the Polish Geological Institute in Warsaw: <http://otworywiertnicze.pgi.gov.pl/Details/Information/>

Thermal modelling was carried out at a regional scale across the entire Polish Basin. Hence, it was necessary to simplify several factors both in geological and methodological aspects such as: (i) Carboniferous strata were selected as the sedimentary basement in the case of the Polish Basin, (ii) the structural-thickness model of Permian to Mesozoic strata and the influence of salt domes. Reconstruction of the thermal history of petroleum source rocks is essential to organic matter maturity predictions. The reconstruction of sediment palaeotemperatures as a function of time and depth requires the specification of heat flow and thermal conductivity values of the rock column. Several heat transfer assumptions were used in our modelling: (1) heat transfer was by conduction, (2) steady-state thermal conditions were used to model heat flow from the base of the sedimentary section to the surface, (3) the heat was assumed to come from the basement but not from radiogenic heat sources within the rocks, (4) the basement heat source was not differentiated between radiogenic heat from the basement and heat from mantle convection. Due to the rifting processes of the MPT (Dadlez et al., 1995; Karnkowski, 1999b; Stephenson et al., 2003; Mazur et al., 2005, 2006) generally higher heat flow values than present-day were assumed for the Permian–Triassic interval, which generally decreased to present-day values. A kerogen Type IIIB kinetic model from Pepper and Corvi (1995) was assigned to the Upper Triassic strata (500 mg HC/gTOC; and 1.0% TOC), whereas the Pepper and Corvi (1995) TIA kinetic model was selected for the Zechstein Main Dolomite horizon (600 mg HC/gTOC; 2% TOC). The kinetic models of hydrocarbon generation selected by Pepper and Corvi (1995) are among the most widely applied in basin modelling studies.

Table 1

A summary table with the lithology and petrophysical properties that were used in the models

Lithology	Density (g/cm ³)	Compressibility (1/Pa)		Thermal conductivity (W/mK)		Heat capacity (cal/gK)	
		Minimum	Maximum	at 20 °C	at 100°C	at 20 °C	at 100°C
DOLOMITE	2.836	10.0	250.0	3.81	3.21	0.202	0.229
EVAPORITE	2.540	1.0	10.0	4.69	3.91	0.194	0.210
EVAPshaly	2.585	10.0	100.0	3.87	3.31	0.200	0.221
LIMEdolom	2.752	10.0	180.0	3.18	2.82	0.198	0.226
LIMEarly	2.707	10.0	300.0	2.63	2.41	0.201	0.235
LIMEsandy	2.695	20.0	700.0	2.93	2.62	0.190	0.219
LIMeshaly	2.700	10.0	550.0	2.51	2.31	0.203	0.237
LIMESTONE	2.710	10.0	150.0	2.83	2.56	0.195	0.223
MARL	2.687	10.0	940.0	2.23	2.11	0.208	0.248
SALT	2.160	1.0	4.0	5.69	4.76	0.206	0.212
SAND&LIME	2.685	15.0	400.0	2.93	2.54	0.186	0.215
SAND&SHALE	2.669	10.0	2.8	2.65	2.38	0.197	0.236
SAND&SILT	2.665	10.0	1.9	2.59	2.31	0.192	0.229
SANDcongl	2.663	10.0	330.0	2.93	2.63	0.184	0.217
SANDshaly	2.666	10.0	1.4	2.78	2.37	0.190	0.226
SANDsilty	2.664	10.0	1.2	2.97	2.64	0.188	0.223
SANDSTONE	2.660	10.0	500.0	3.12	2.64	0.178	0.209
SHALE	2.680	10.0	60.0	1.98	1.91	0.213	0.258
SHALE&LIME	2.695	20.0	1.5	2.39	2.24	0.208	0.246
SHALE&SAND	2.669	10.0	2.8	2.65	2.38	0.197	0.236
SHALE&SILT	2.674	10.0	13.0	2.09	1.97	0.207	0.251
SHALEcalc	2.688	10.0	5.0	2.22	2.09	0.208	0.248
SHALEcarb	2.655	10.0	45.0	1.50	1.43	0.212	0.258
SHALEcoal	2.474	10.0	16.5	1.80	1.60	0.202	0.244
SHALEevap	2.630	10.0	7.0	2.93	2.61	0.210	0.247
SHALEsand	2.674	10.0	9.0	2.32	2.12	0.205	0.248
SHALEsilt	2.677	10.0	25.0	2.05	1.94	0.210	0.254
SILT&SAND	2.665	10.0	1.9	2.59	2.31	0.192	0.229
SILT&SHALE	2.674	10.0	13.0	2.09	1.97	0.207	0.251
SILT sandy	2.666	10.0	3.0	2.55	2.33	0.192	0.230
SILTshaly	2.675	10.0	15.0	2.09	1.98	0.203	0.245
SILTSTONE	2.672	10.0	8.0	2.14	2.03	0.201	0.242

In lithology types the following system was applied for abbreviations: e.g., SANDcongl (first lithology in upper case and second in lower case) – 70% sandstone and 30% of conglomerate; SAND&SHALE (both lithologies in upper case) – 50% sandstone and 50% shale

RESULTS

BURIAL AND THERMAL HISTORY

The first part of the thermal maturity modelling involved reconstruction of the Late Paleozoic to Cenozoic burial and thermal history, which was necessary for further hydrocarbon generation modelling. However, the quality of the VR data in many boreholes is varied, which means that in many cases thermal history models are not unique and alternative models are possible (e.g., Majorowicz et al., 1984; Karnkowski, 1996, 1999b; Poprawa et al., 2005; Zielinski et al., 2012). In this 1-D petroleum system modeling study, burial and thermal history models were applied (adopted) based on the best-fit models published by Resak et al. (2008) for Pomerania, Botor (2011) for the Kujawy and northern Fore-Sudetic Homocline (FSH), as well as Kozłowska and Poprawa (2004) and Kuberska et al. (2021) for the Masovia area, and Botor (2011), Botor et al. (2013), and partially (for the eastern FSH), Poprawa et al. (2005) and Maćkowski (2005) for the FSH, as well as Botor et al. (2019a)

for the EEC area. Details of the burial and thermal history as well as petroleum generation characteristics in the Paleozoic (Ediacaran to Carboniferous) source rocks was given by Botor et al. (2013) and Botor et al. (2019a, b). Detailed discussion concerning burial and thermal history, model calibration and sensitivity analysis has already been carried out in these papers, and is not repeated here. Herein, burial and thermal history is only summarized at a regional scale in the context of further hydrocarbon generation modelling of the Zechstein Main Dolomite and Upper Triassic source rocks. The most important and typical examples of burial and thermal history are given in Figure 5, while examples of model sensitivity analysis are given in Figure 6. Because most boreholes were drilled to reach the Carboniferous, models were constructed including the Carboniferous. However, these models also show Permian to Cenozoic geological evolution, including the Zechstein Main Dolomite and Upper Triassic source rocks.

A sensitivity analysis was carried out to investigate the effects of changes in heat flow (HF) and different extents of erosion during the most decisive phases of burial and subsequent

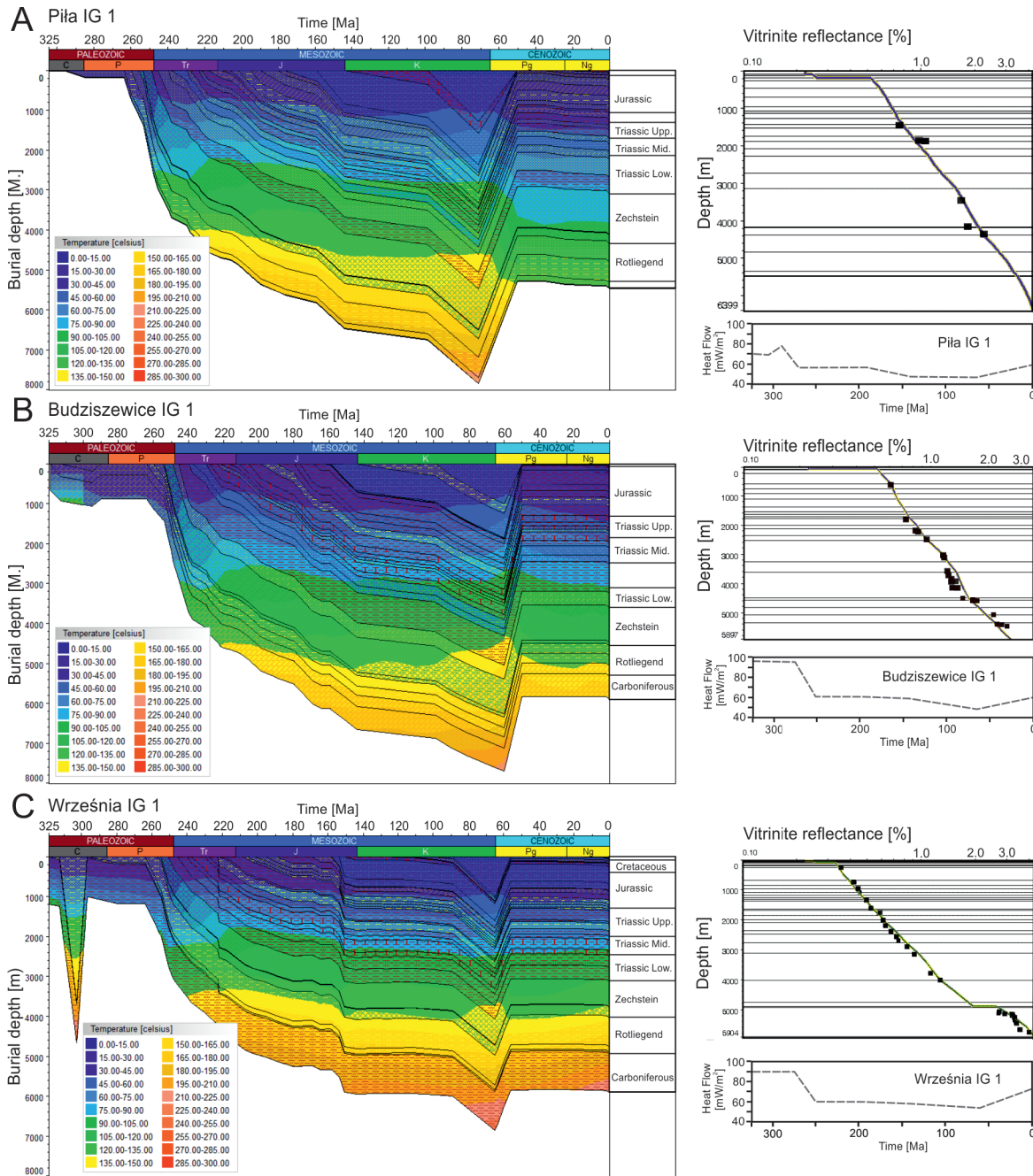


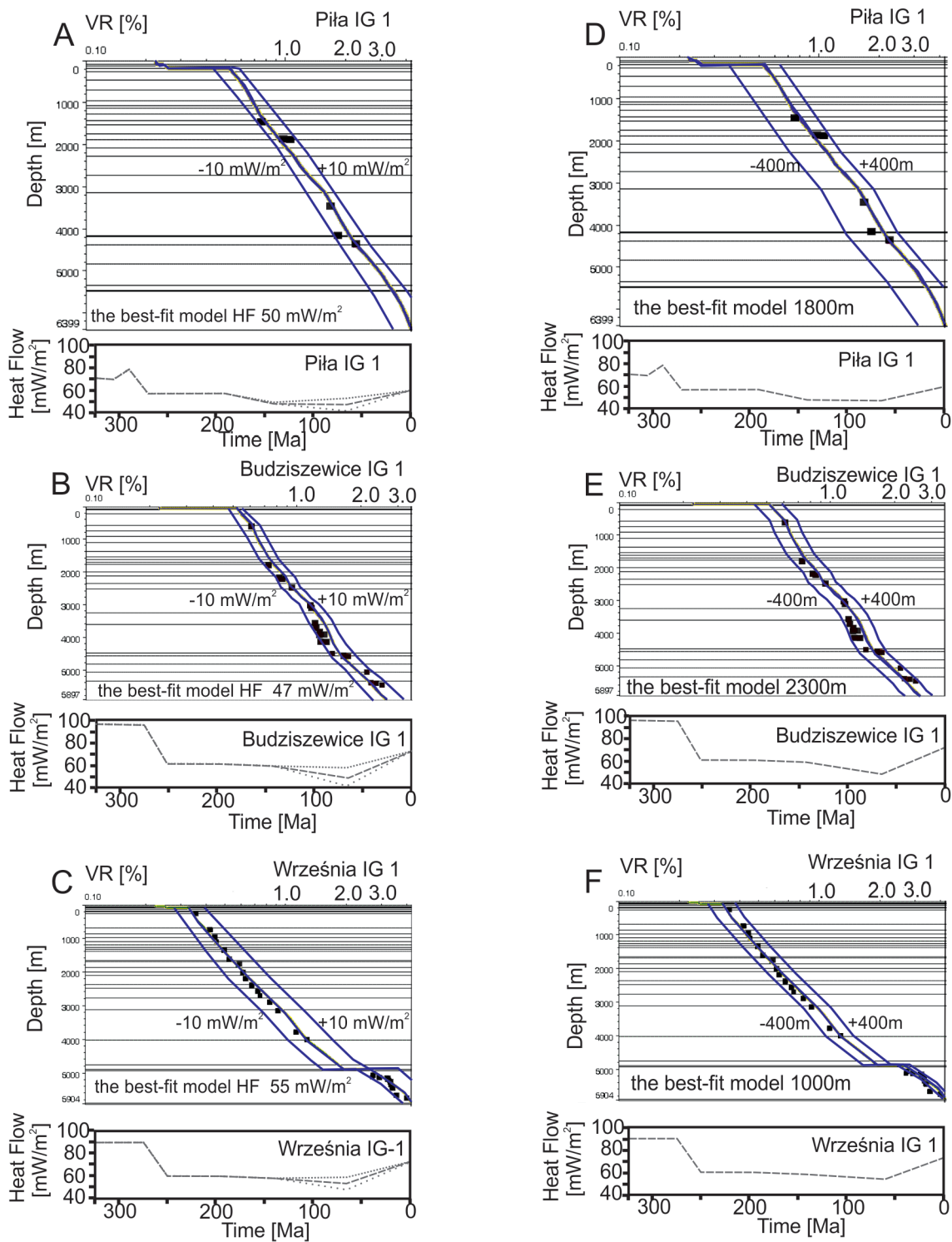
Fig. 5. Burial and thermal history models of selected boreholes

A – Piła IG 1, **B** – Budziszewice IG 1, **C** – Września IG 1 (modified based on Botor, 2011; Botor et al., 2013); calibration for the best-fit models are also given with measured vitrinite reflectance and heat flow development

exhumation in the Late Cretaceous (Fig. 6). Figure 6A, B, C shows the variation in heat flow in 10 mW/m² steps from the best-fit scenario. The best-fit scenario assumes high heat flows at times of extensional tectonics, decreasing during subsidence and finally increasing after tectonic inversion to present-day values (Fig. 5). Such a HF scenario was used in previous studies summarized by Botor (2011) and Botor et al., (2013, 2019a). To illustrate the effect of changes in palaeo-heat flow, different heat flow values during maximum burial were tested during the most sensitive time of the Late Cretaceous. By increasing the heat flow values of 10 mW/m² or higher during maximum burial in Late Cretaceous times (Fig. 6A, B, C), calculated VR values are too high compared to measured data. Respectively, by decreasing the heat flow values of 10 mW/m² or lower during the

same burial phase, calculated VR values are too low compared to measured data. Secondly, the influence of the removed sediment thickness was assessed (Fig. 6D, E, F). This was performed by adjusting the thickness of eroded sediment during the maximum burial and erosion phase in the Late Cretaceous to Early Paleogene. The assumption of eroded sediment thicknesses of above or below 400 m different than the best-fit models cause significant change in the calculated VR curve. In such cases, the calculated VR curve is unacceptable, being outside the measured VR values. Further details of sensitivity analysis models were published by Botor (2011).

In the area of the Polish Basin analysed, burial history was characterised by relatively continuous subsidence from the Permian to Late Mesozoic (Fig. 5). However, there were two



- - - -10 mW/m² heat flow during maximum burial
 ——— heat flow in the best-fit model
 - - - +10 mW/m² heat flow during maximum burial

VR [%] vitrinite reflectance

Fig. 6. Sensitivity analysis for selected models in the study area

A–C – models show change in thermal maturity due to change of heat flow ± 10 mW/m² during maximum burial in the Late Cretaceous. In these models the amount of erosion of the Late Mesozoic was unchanged compared to the best-fit models (from Fig. 5). In the **D–F** models heat flow in the Late Cretaceous was equal to the best-fit models, whilst the amount of sediment thickness removed due to tectonic inversion in the Late Cretaceous was adjusted

major intervals of uplift and erosion: (1) in the Late Carboniferous to Early Permian and (2) in the Late Cretaceous/Paleogene. The first interval is difficult to quantify due to high rates of burial in the Mesozoic, while the second one resulted in removing 200 m to 3 km of Mesozoic strata (Botor et al., 2013, 2019a). The highest values occurred along the axis of MPT, lowering towards the flanks. The Cenozoic interval did not significantly influence burial history due to the low stratal thickness, not exceeding 350 m (Piwocki, 2004). The best-fit calibration (i.e. the best fit between the measured and calculated VR values) has been achieved by means of applying increased heat flow values ($\sim 95 \text{ mW/m}^2$) in the Carboniferous–Early Permian interval, probably related to volcanic processes and some hydrothermal activity in the study area. The Late Permian–Mesozoic and Cenozoic interval was characterized by moderate heat flow in the range $50\text{--}80 \text{ mW/m}^2$. The lowest HF was in the Cretaceous ($40\text{--}48 \text{ mW/m}^2$) before tectonic inversion, after which HF increased to the present-day value (Botor, 2011, Botor et al., 2013, 2019a).

In the Polish Basin, the Permian and Triassic strata reached maximum thermal maturity of organic matter during the Mesozoic. Thermal maturity of the Carboniferous organic matter was reached before the Permian particularly in the eastern FSH i.e., the area between boreholes Września IG 1 and Dankowice IG 1, which is supported by the break in the VR profile in boreholes (Botor et al., 2013). This was related probably to the large amount of eroded sediments ($>3 \text{ km}$) and high heat flow values ($\sim 100 \text{ mW/m}^2$), or was caused by a fluid flow event. On the other hand, in the MPT area, and in the zone of marginal troughs on both sides of the MPT, much more complicated thermal maturity patterns, which were developed during the Mesozoic burial, are found (Botor, 2011; Botor et al., 2013, 2019a). In the southern part of the Polish Basin, a higher thermal palaeogradient was found locally in Jurassic. This suggests the presence of an additional thermal event in the Early–Middle Jurassic, characterized by a strongly increased heat flow (Poprawa and Grotek, 2004). This phenomenon was likely associated with a phase of extensive tectonic activity in this part of the basin (Kutek, 1994). The calculated heat flow reaches very high values, up to over $\sim 100 \text{ mW/m}^2$, and this anomaly in individual borehole sections expires relatively quickly (e.g., Zielinski et al., 2012; Botor et al., 2013). Modelling does not make it possible to unequivocally state whether this anomaly is related to perturbations of the conductive heat flow, or whether it results from convective heat transport. Farther towards the SE, in the southern part of the Masovian Trough and in the northern part of the Lublin area, such a phenomenon was documented using modelling based on both VR data and the results of illite K-Ar dating (Kozłowska and Poprawa, 2004; Kuberska et al., 2021). This event was roughly simultaneous with a phase of extensive or transient tectonic reactivation of the Polish Basin (Dadlez et al., 1995). The development of the Polish Basin ended with the Late Cretaceous–Early Paleogene tectonic inversion, which led to intense erosion of the sedimentary infill of the basin, reaching the Jurassic and, locally, even the Upper Triassic (e.g., Botor et al., 2013).

The depth of maximum burial, which occurred in the Late Cretaceous, of both Zechstein Main Dolomite and Upper Triassic source rocks varies in different parts of the Polish Basin. (Figs. 7 and 8). The highest values were calculated along the MPT axis. These values decrease towards the basin flanks. Maximum burial of the Zechstein Main Dolomite source rocks was 5–7 km in the MPT area (i.e., the area between the boreholes Czaplonek IG 2 and Budziszewice IG 1), decreasing to 2–3 km towards NE and SW (Fig. 7). The shallowest burial ($<1.5 \text{ km}$) was in the most eastern and NE areas (i.e.,

Bartoszyce IG 1, and Żebrak IG 1). Maximum burial of the Upper Triassic source rocks ($>6 \text{ km}$) occurred in the area of boreholes Krośniewice IG 1 – Poddębice IG 1 – Zgierz IG 1, in the MPT area (Fig. 8). These values decrease towards the basin's flank similarly as in Zechstein Main Dolomite. The lowest values ($<1 \text{ km}$) also occurred in the NE and the easternmost areas (Bartoszyce IG 1, and Żebrak IG 1).

In the case of the Pomeranian segment of the Polish Basin, the reconstruction of a coherent, regional scale thermal history is difficult. This relates to the differences between the variants of heat flow changes over time, optimal for the individual boreholes analysed, and the lack of thermal maturity data that would fully cover the profiles of the boreholes analysed (Resak et al., 2008; Botor et al., 2013). This applies in particular to the southern part of the Pomeranian segment of the MPT, where lateral differences in thermal history may be related to halokinetic activity, leading to strong lateral thermal conductivity anisotropy. In the Pomeranian Swell the burial history is mostly characterized by relatively rapid subsidence from the Permian to Triassic or Jurassic followed by slower subsidence in the Cretaceous (Fig. 5). In the Late Cretaceous/Paleogene a rapid phase of uplift took place. The former event marks the setting up of the MPT depocentre and is associated with considerable crustal extension (Dadlez et al., 1995). Between Early Triassic and Late Cretaceous the area subsided almost continuously, and burial was interrupted only by insignificant erosional events resulting from salt doming in the Late Triassic. After the Early Triassic, sedimentation rates were much lower, particularly in the latest Triassic and Cretaceous. Finally, Late Cretaceous/Paleogene uplift resulted in the removal of 300–700 m of deposits. The heat flow was $\sim 30\text{--}50 \text{ mW/m}^2$ during this time (Botor et al., 2013). During the latest Carboniferous to Early Triassic, heat flows were assigned to be $\sim 55\text{--}95 \text{ mW/m}^2$ (Botor et al., 2013). These higher values are due to the assumed rifting origin of the MPT (Dadlez et al., 1995). However, it is difficult to assess heat flow evolution for this interval because of high Mesozoic burial, which caused overprinting of the Variscan VR response. Further details of burial and thermal history are given in Resak et al. (2008) and Botor et al. (2013).

In the central part of the MPT, burial history was also characterized by very rapid subsidence in the Late Permian to Early Triassic, followed by slower subsidence from the Late Triassic to Cretaceous. Finally, Mesozoic subsidence was interrupted by Late Cretaceous/Paleogene uplift, which caused erosion of variable amounts of the Late Mesozoic succession (from a few metres to 3 km as in the case of Budziszewice IG 1). Due to very substantial Mesozoic burial it is difficult to assess heat flow ($\sim 60\text{--}110 \text{ mW/m}^2$) in the Carboniferous to Early Permian (Botor, 2011). Further details of the burial and thermal history of this area are given in Botor (2011) and Botor et al. (2013).

In the eastern part of the Polish Basin (Masovia), the local burial history is characterized by more or less continuous subsidence from the end of the Carboniferous to the end of the Cretaceous. Acceleration of subsidence rate is inferred in the Late Permian to Early Triassic, and Late Jurassic and Late Cretaceous. The major period of uplift and erosion was in the Latest Carboniferous to Early Permian, while the Late Cretaceous/Paleogene uplift was not significantly marked in this area (Botor et al., 2013, 2019a). Thermal history models in the Masovia area assume a short-lived hydrothermal (?) Jurassic event in order to achieve the best fit between measured and calculated VR, as was suggested by Kozłowska and Poprawa (2004), Zielinski et al. (2012) and Kuberska et al. (2021).

The area east of the TTZ on the slope of the EEC shows a similar subsidence pattern; however, the burial depth is lesser to the NE, because this was an area located in the marginal part

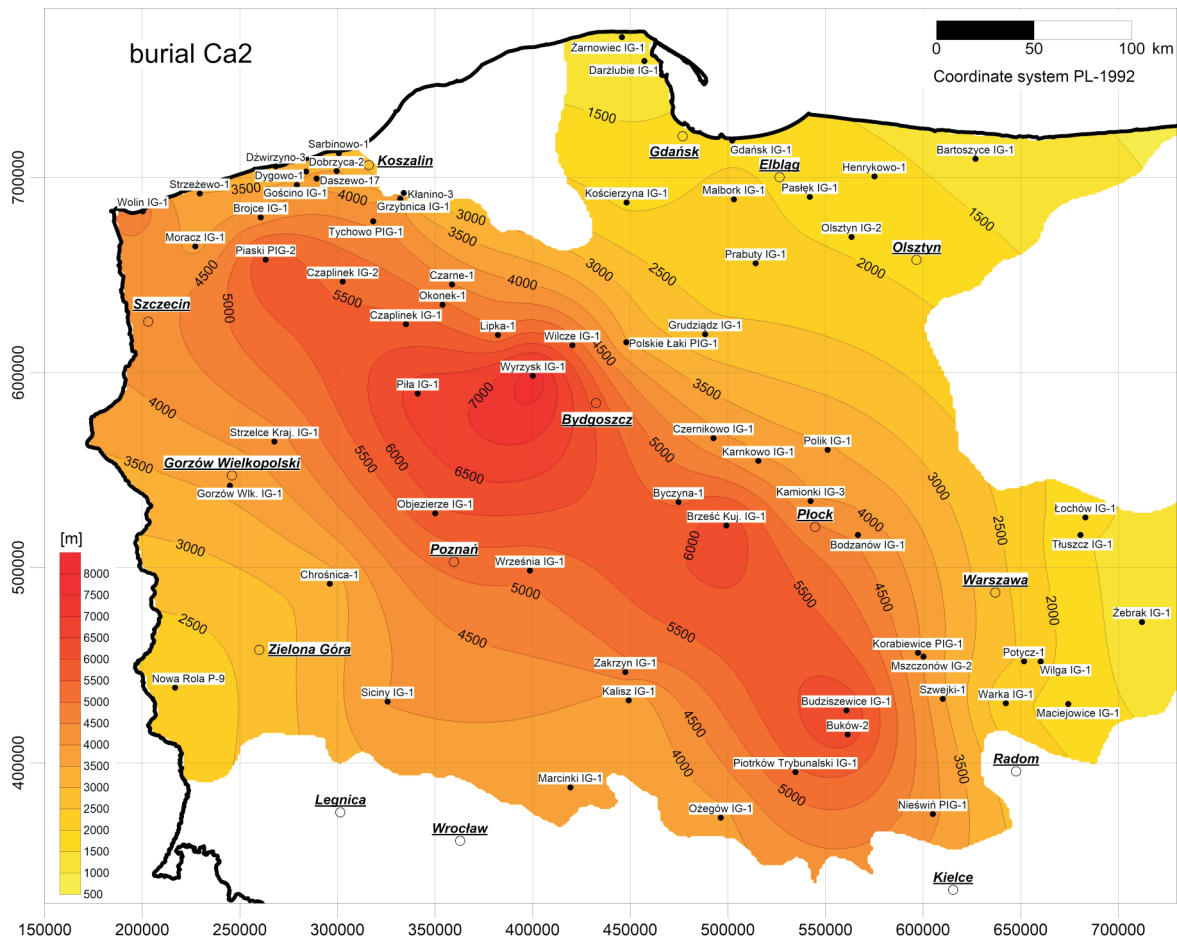


Fig. 7. Calculated maximum burial depth pattern before Late Cretaceous inversion for the Zechstein Main Dolomite

The coordinate system used in Figures 7–12 is – Poland 1992 that is based on the ETRS89 datum, GRS80 spheroid and the Transverse Mercator projection with 19°E as a central meridian; extent and facies of Zechstein Main Dolomite modified based on Wagner (1994), Dadlez et al. (1998), Peryt et al. (2010)

of the Permian–Mesozoic basin of Central Poland (Botor et al., 2019a, b). The Cenozoic deposits, due to their very small thickness and variable distribution in the research area, do not significantly affect the burial patterns of the Permian and Mesozoic succession.

THERMAL MATURITY

Thermal maturity of organic matter was calculated as mean random vitrinite reflectance applying the Sweeney and Burnham (1990) algorithm, which is still valid in most cases (Burnham et al., 2016). The vitrinite reflectance map has been calculated for the bottom of the Zechstein Main Dolomite (Fig. 9) and the bottom of the Upper Triassic (Fig. 10). These maps are based on 1-D models accomplished for four development steps: (a) Late Triassic (~200 Ma), (b) Late Jurassic (144 Ma), (c) Late Cretaceous (65 Ma), and (d) the present-day. The VR pattern for both the Zechstein Main Dolomite and Upper Triassic source rocks is generally related to the maximum burial and development of the MPT. The highest values are generally observed along the axial part of the Polish Basin. The present-day VR map of the Zechstein Main Dolomite and Upper Triassic (Figs. 9D and 10D) shows an almost identical distribution to the Late Cretaceous pattern (Figs. 9C and 10D). This allows the assumption that the recent VR pattern of the Zechstein Main Dolomite and Upper Triassic was developed in the Meso-

zoic, finally reaching its VR pattern in the Late Cretaceous. The fastest thermal maturity development occurred in the central part of the MPT, where VR reached >1.3 % in the Late Triassic in the Zechstein Main Dolomite source rocks. Further increase in VR was in the Late Cretaceous when the Zechstein Main Dolomite source rocks reached VR values of >1.3 % along the axis of the MPT, from the Czaplinek IG 2 to the Nieświn PIG 1 boreholes. In the Upper Triassic source rocks, thermal maturity reached >0.7% VR close to the Holy Cross Mountains (Nieświn PIG 1 – Piotrków Trybunalski IG 1 area) in the Late Jurassic. In the Late Cretaceous, maximum VR values were reached in the central part of the MPT between the boreholes Krośniewice and Budziszewice IG 1 (Fig. 10). The VR values in the area of petroleum occurrence in the Zechstein Main Dolomite reservoirs is in the range ~0.5 to 1.3 %.

HYDROCARBON GENERATION

Final results of the hydrocarbon generation modelling have been shown as a kerogen transformation ratio (%TR), which characterizes very well the development of these processes (Figs. 11 and 12). TR calculated values are given at the bottom of the Zechstein Main Dolomite and Upper Triassic strata. As TR development is similar to VR development, only the final stage for the Late Cretaceous was shown, which is equal to the present-day pattern. Hydrocarbon generation development re-

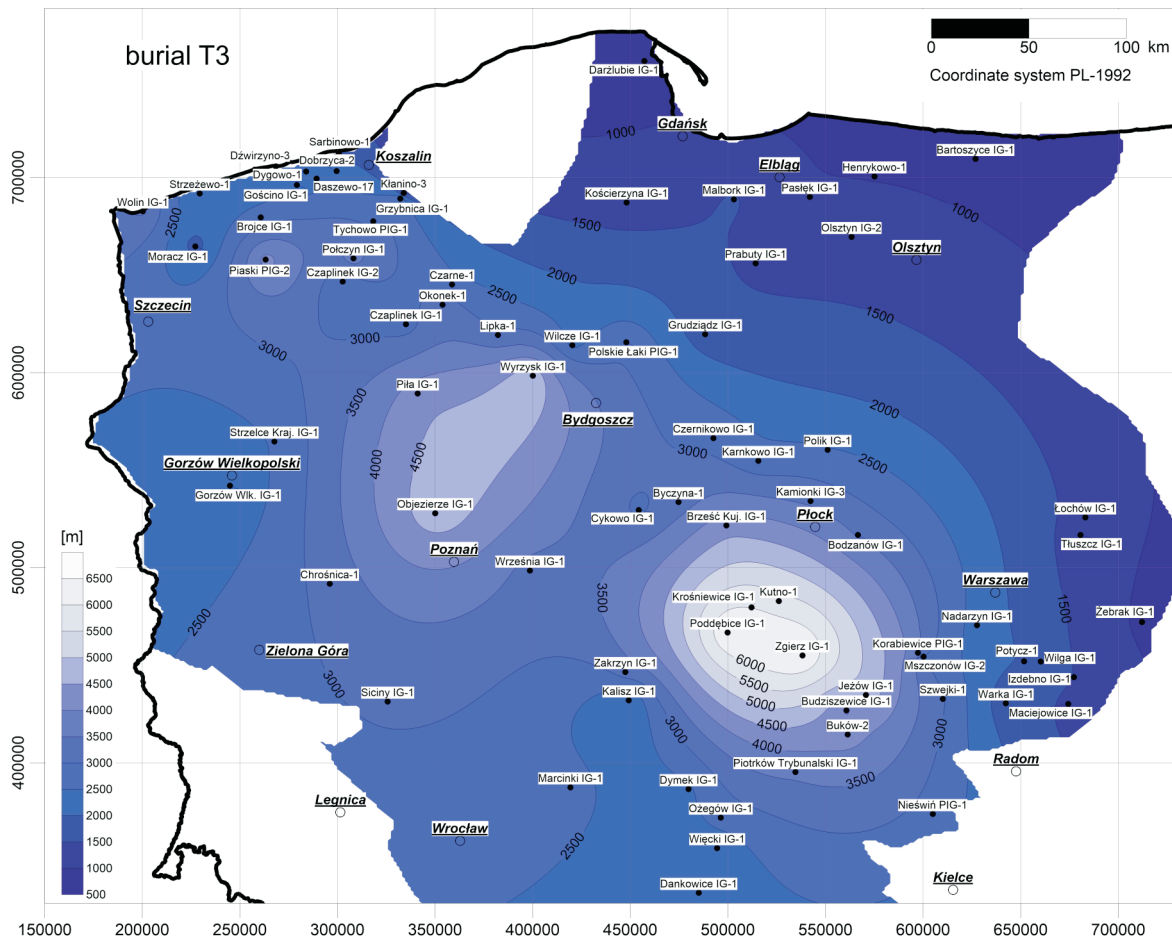


Fig. 8. Calculated maximum burial depth pattern before Late Cretaceous inversion for the bottom of the Upper Triassic strata

Extent of Upper Triassic modified based on Dadlez et al. (1998) and Feist-Burkhardt et al. (2008)

veals considerable variation among particular Zechstein Main Dolomite and Upper Triassic basin zones. *TR* reached different values in the range ~10 to 100 % (Figs. 11 and 12). The highest *TR* values occur in the zones of the maximum maturity of the organic matter (Figs. 9 and 10). The Zechstein Main Dolomite source rocks area with 90% *TR* includes most of the Zechstein Main Dolomite basin. This area occurs along the axis of the MPT and FSH. Lower *TR* values are calculated outside of this area towards the east. The lowest values are on the slope of the EEC (Fig. 11). The hydrocarbon generation processes took place in several pulses during the Mesozoic, principally from the Middle–Late Triassic up to the Late Jurassic and in the Cretaceous. In the FSH, the Zechstein Main Dolomite source rocks entered the oil window in the Late Triassic to Early Jurassic with burial to 2 km (Fig. 5). The end of intense generation was in the Late Jurassic; however, generation was still active until the Late Cretaceous. In Pomerania, the source rocks entered the oil window from the Mid-Triassic to the Cretaceous when the burial depth was >2.5 km. Late generation took place until the Late Cretaceous. Hydrocarbon migration was of short distance in the FSH, because most petroleum deposits occur in the area of high *TR* (40–90 % *TR*; Fig. 12). Whereas, in the Pomerania and central part of the Polish Basin, hydrocarbon migration distance seems to be longer since many petroleum deposits occur in zones of lower *TR* (10–50 % *TR*; Fig. 12). The Upper Triassic source rocks entered the oil window in the Jurassic, and hydrocarbon generation was completed in the Late Cretaceous with

tectonic inversion of the Polish Basin. *TR* in the Upper Triassic source rocks is generally lower than in the Zechstein Main Dolomite due to lesser burial. In the Upper Triassic source rocks the highest *TR* values (>50 %) are calculated along the MPT axis, in the area between boreholes Piła IG 1 and Piotrków Trybunalski IG 1 (Fig. 12). The most pronounced zone is in the Krośniewice Trough (i.e., Krośniewice IG 1 to Budziszewice IG 1 area), where locally *TR* reached >90%.

DISCUSSION

BURIAL AND THERMAL HISTORY

Generally, the 1-D basin modelling performed supports earlier studies dealing with the tectonic development of the Polish Basin. The Permian and Mesozoic strata in the Polish Basin rest on the older Paleozoic, the genesis of which is connected with the development of rifting in the Early Permian (Dadlez et al., 1995; Karnkowski, 1999b; Kutek, 2001). Deposition of the Permian strata was within the period of relatively rapid subsidence, continuing through the Late Permian and Early Triassic (Dadlez et al., 1995). This event is correlated with a tectonic phase commonly observed in the Polish Basin and interpreted as a syn-rift phase (Dadlez et al., 1995). Then, for most of the Triassic, Jurassic, and Early Cretaceous, subsidence related to the rift phase of thermal subsidence was maintained (Dadlez et

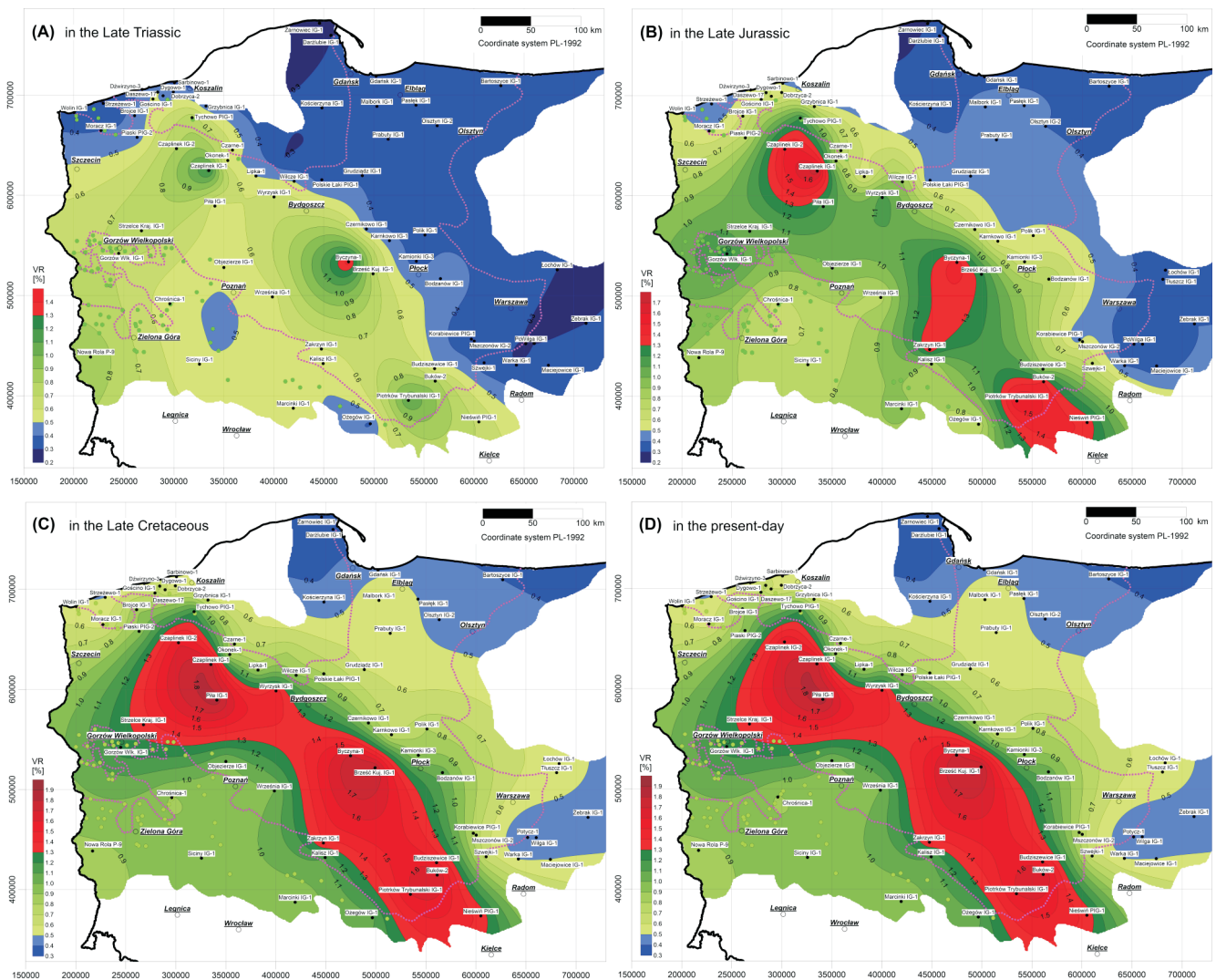


Fig. 9. Calculated thermal maturity and hydrocarbon window development of the Zechstein Main Dolomite

A – in the Late Triassic, B – in the Late Jurassic, C – in the Late Cretaceous, D – present-day; VR - vitrinite reflectance; blue – immature zone, green – oil window, red – gas window; dotted magenta line shows platform/barriers extent *versus* the current extent of the Zechstein Basin (modified based on Wagner, 1994, Dadlez et al., 1998; Peryt et al., 2010); green dots represent oil and gas fields in the Zechstein Main Dolomite

al., 1995; Karnkowski, 1999b; Kutek, 2001). In the Late Cretaceous, in the area investigated, tectonic reactivation took place, expressing accelerated subsidence in a compressional tectonic regime (Dadlez et al., 1995; Krzywiec, 2002). Taking into account the evolution of the Polish Basin at this time, it can be inferred that this process took place in a compressional tectonic regime (Dadlez et al., 1995; Krzywiec, 2002), and the end of the Cretaceous tectonic inversion took place (Dadlez et al., 1995; Krzywiec, 2002; Resak et al., 2008, 2010).

In most 1-D models, the best-fit calibration was achieved by applying increased heat flow values in the Permian and Early Triassic intervals (Poprawa and Grotek 2004; Poprawa et al., 2005; Resak et al., 2008; Botor, 2011, Botor et al., 2013), assumed to be due to rifting of the MPT (Dadlez et al., 1995; Karnkowski, 1999b; Stephenson et al., 2003; Mazur et al., 2005, 2006). Generally, subsidence analyses show an initial syn-rift phase of MPT development from the Permian to Early Triassic and an increase in subsidence in the Late Jurassic as

well as in the Cenomanian (Dadlez et al., 1995; Stephenson et al., 2003; Resak et al., 2008). The development of the Polish Basin was completed by Late Cretaceous and/or Early Paleogene tectonic inversion, as in the other basins of the Central European basin system (Doornbal and Stevenson, 2010; von Eynatten et al., 2021). The sedimentary deposits were eroded down to the Lower Jurassic or Upper Triassic, whereas elongated troughs at the flanks are characterized by a thick Upper Cretaceous succession (e.g., Mazur et al., 2006). Generally, heat flow evolution in this study assumes higher than present-day heat flow values in Carboniferous to Triassic time due to rifting of the MPT (Dadlez et al., 1995), and decreasing heat flow values to the present day. Slightly lower than present-day heat flow was assumed for the Cretaceous in the axial part of the MPT. Additionally, an increase in heat flow occurred in the eastern part of the MPT in the Jurassic, as suggested by diagenetic studies by Kozłowska and Poprawa (2004), Zielinski et al. (2012) and Kuberska et al. (2021).

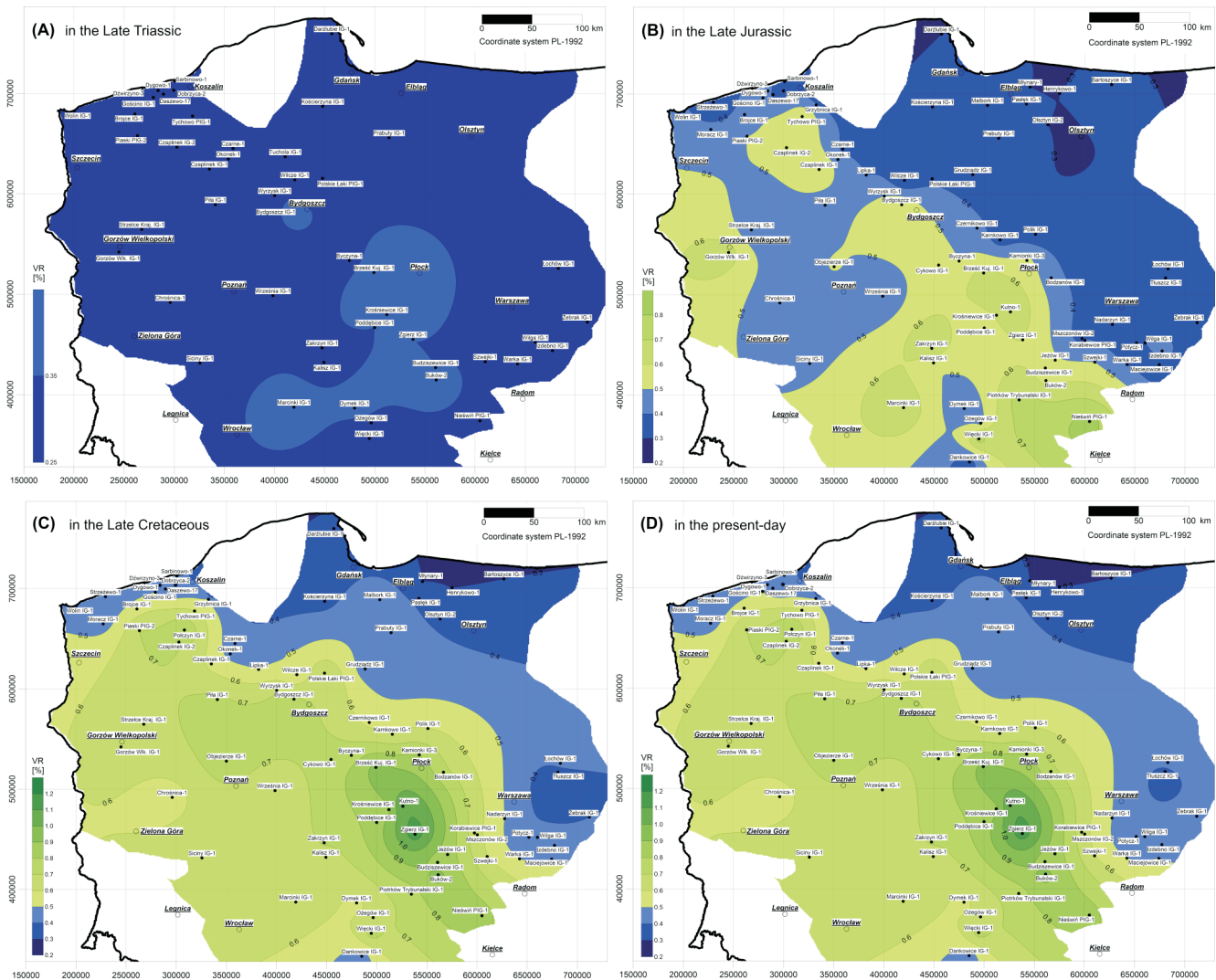


Fig. 10. Calculated thermal maturity and hydrocarbon window development for the bottom of the Upper Triassic

A – at the end of Late Triassic, B – in the Late Jurassic, C – in the Late Cretaceous, D – present-day; VR – vitrinite reflectance; blue – immature zone, green – oil window

During the Permian and Mesozoic, the area east of the TTZ was located in the marginal part of the Polish Basin that overlapped the SW slope of the EEC (e.g., Kutek and Głazek, 1972; Pożaryski and Brochwicz-Lewiński, 1978; Dadlez et al., 1995; Kutek, 2001). A characteristic feature of the SW slope of the EEC is an increasing thickness of deposits towards the TTZ. Up to a few kilometres of strata were deposited at that time, and the thickness rapidly decreases from the axis of the MPT towards the interior of the EEC and towards the FSH. In contrast to the MPT, where significant Late Cretaceous basin inversion took place (Botor et al., 2018; Łuszczak et al., 2020), the part of the Polish Basin extending NE over the TTZ and adjacent area of the EEC experienced only mild inversion (e.g., Krzywiec, 2009; Krzywiec et al., 2017a, b).

Independent premises for the occurrence of a lowered thermal gradient (i.e. lower heat flow) in the Late Cretaceous zone along the MPT were obtained from thermochronological apatite fission-track data (Poprawa and Andriessen, 2006). In the area of EEC east of the TTZ, a recently accomplished thermo-chronological study of Botor et al. (2021) supplemented by earlier work of Kowalska et al. (2019) based on K-Ar dating and clay minerals and produced a more reliable thermal history of this area. The Mesozoic thermal history of the SW slope of the

EEC area was characterised by gradual cooling from peak temperatures ($>120^{\circ}\text{C}$) at the transition from the Triassic to Jurassic due to decreasing heat flow (Botor et al., 2021). This result is probably representative for the entire TTZ area, as comparable results were obtained by Schito et al. (2018) in the Ukrainian part of the EEC, who postulated that exhumation through the $40\text{--}120^{\circ}\text{C}$ temperature range took place between the Late Triassic and Early Jurassic, and that no significant burial occurred afterwards. The data of Botor et al. (2021) are consistent with decreasing heat flow during the Mesozoic (particularly within the Cretaceous) as suggested by Poprawa and Andriessen (2006) along the axis of the MPT. The elevated Permian-Triassic heat flow was probably a consequence of early Permian continental rifting. The decrease in post-Permian heat flow appears an important cause of Late Mesozoic cooling. The thermal models show mostly gradual cooling with little effects of the Late Cretaceous basin inversion along the EEC. Apatite fission-track data did not record any cooling acceleration, which can be attributed to tectonic inversion in the Late Cretaceous (Botor et al., 2021). This is related to the fact that tectonic inversion was significantly weaker in the part of the Polish Basin overlapping the EEC (Krzywiec et al., 2017b).

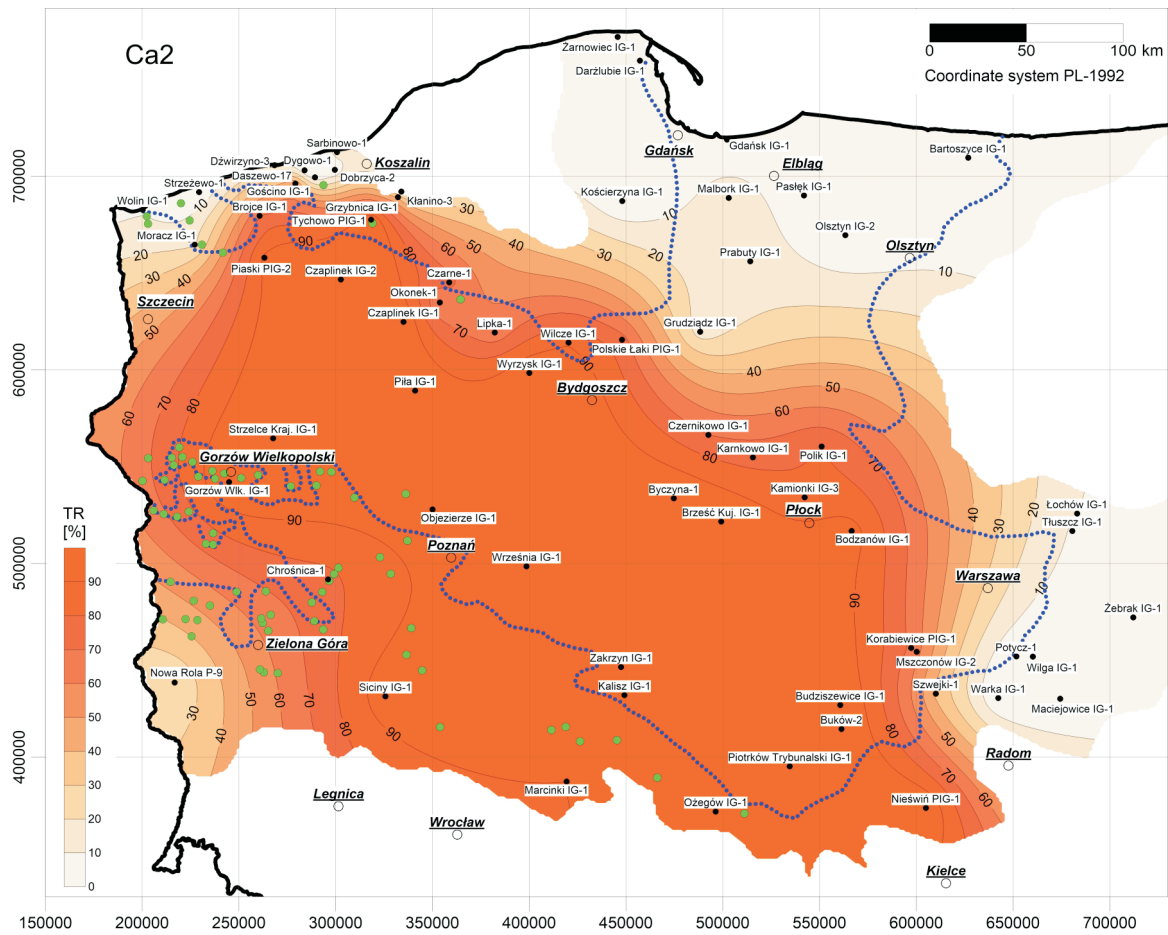


Fig. 11. Calculated kerogen transformation ratio of the Zechstein Main Dolomite in the Late Cretaceous

TR – kerogen transformation ratio; dotted blue line shows platform/barriers extent versus the current extent of the Zechstein Basin (modified based on Wagner, 1994, Dadlez et al., 1998; Peryt et al., 2010); green dots represent oil and gas fields in the Zechstein Main Dolomite

HYDROCARBON GENERATION

In the Polish Basin, the results of the maturity modelling performed indicates that several stages of development of hydrocarbon generation in the Permian and Triassic strata may be distinguished. Permian source rocks attained their maximum thermal maturity between the Late Triassic and Cretaceous. The Upper Triassic source rocks generated hydrocarbons in the Jurassic to Late Cretaceous, mainly in the Krośniewice trough and adjacent area of the MPT. This area had also been suggested earlier, due to high burial rates, as the main hydrocarbon generation “kitchen” (Bachleđa-Curuś and Semyrka, 1990; Kosakowski et al., 2015).

The Zechstein Main Dolomite source rocks generated hydrocarbons in several phases during the Mesozoic until Late Cretaceous, which is also supported by the wide occurrence of hydrocarbon fields in the Zechstein Main Dolomite rocks. The degree of transformation of the Zechstein Main Dolomite kerogen corresponds with the initial and main phases of liquid hydrocarbon generation in the area of the EEC, particularly in the Masovia areas and in northern Pomerania. In the axial part of the MPT and in the FSH, the kerogen is characterized by a transformation degree that corresponds with the main phases of liquid hydrocarbon, the phase of gas condensate generation, as well as the phase of thermogenic dry gas generation which is in agreement with the findings of Karnkowski (1996, 1999b).

The modelling performed supports also the results of Pletsch et al. (2010), suggesting that petroleum generation in basinal deposits of the Zechstein Main Dolomite started during the Early Triassic, at burial depth >1700 m. The Zechstein Main Dolomite source rocks entered the oil window in the Late Triassic (basinal deposits) with burial to 2000 m, and in the Early Jurassic (platform deposits) with burial to 1800–2200 m. The end of generation was in the Late Triassic (basin) and in the Middle Jurassic (platform). In NW Poland, the Zechstein Main Dolomite source rocks in Pomerania reached the early generation phase during the Early Triassic (axial part of the basin) and the Late Triassic (platform deposits). Early generation started at burial depths of >2500 m. The source rocks entered the oil window from Mid-Triassic to Cretaceous times when the burial depth was >2700 m burial depth. Late generation took place from the Early Triassic in the basin to the Late Cretaceous on the slope and platform, when the petroleum potential of kerogen from the Zechstein Main Dolomite source rocks became exhausted (Pletsch et al., 2010).

UNCERTAINTY OF TRANSFORMATION RATIO

The extent of the advance of hydrocarbon generation in source rocks in this work is presented as the kerogen transformation ratio. The TR depends essentially on the thermal matu-

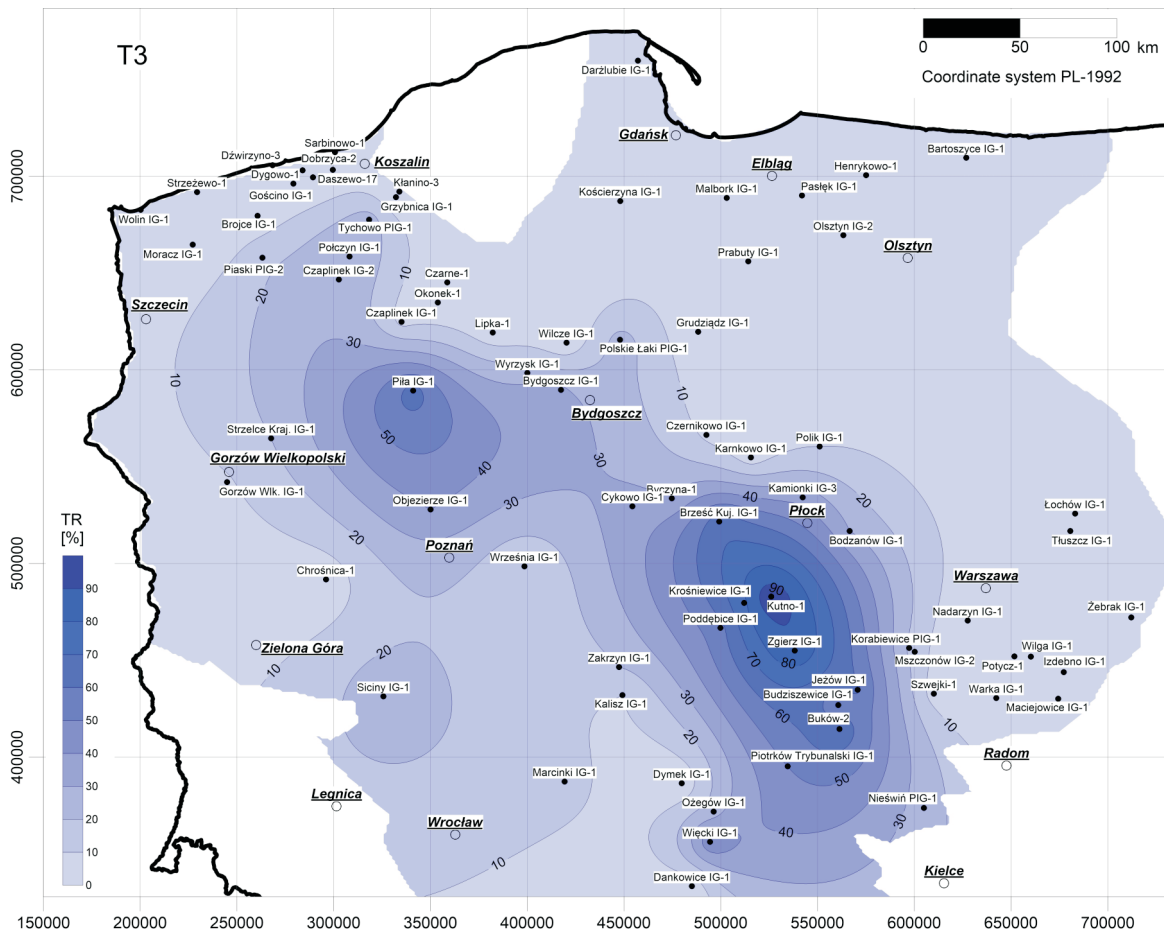


Fig. 12. Calculated kerogen transformation ratio development of Upper Triassic strata (for the bottom of the Upper Triassic, T3) in the Late Cretaceous

TR – kerogen transformation ratio

richness of the organic matter, although a number of factors also influence it. As a result, the relation of thermal maturity and burial depth to *TR* is not always simple and unambiguous (Aguilera, 2018). It seems that *TR* variation most likely reflects organic facies variations of the source rock, as each organic facies has a different transformation ratio behaviour caused by its chemical kinetics. In this work the most widely used kinetic model of Pepper and Corvi (1995) was applied. However, other kinetic models could give slightly different results (Hantschel and Kauerauf, 2009). Therefore, further research on this topic should start from detailed assessment of chemical kinetics reactions. In this work the *TR* pattern is based on the assumption of homogeneous distribution of organic matter in the source rock. However, variations in *TR* could be interpreted in terms of different organofacies in the source rock, stratigraphic variations (sequence stratigraphy), and varying depositional and preservation conditions of the organic matter (Tyson, 2001, 2005; Katz, 2005; Hantschel and Kauerauf, 2009). The hydrocarbon potential of the source rock is mainly controlled by the total organic carbon content, type, and maturity of the organic matter (Hunt, 1996; Bohacs et al., 2005). One of the main uncertainties in petroleum system analysis is the distribution of organic matter within the source rock, both in terms of quantity (TOC) and quality (hydrogen index, HI). Reliable assessment of the organic matter quality is crucial for evaluating hydrocarbon generation/expulsion scenarios. Variations in source-rock richness

and quality are the least well-known variables (e.g., Tyson, 2001; 2005; Katz, 2005; Hantschel and Kauerauf, 2009). In basin modelling, a conceptual approach or simple models applying average geochemical values describing source rock properties are widely used (Hantschel and Kauerauf, 2009). However, these are often insufficient, particularly in areas with heterogeneous geological conditions and/or reflecting variable depositional environments. The basic problem in hydrocarbon potential assessment is that mostly present-day values of TOC and HI are used, causing underestimation of initial hydrocarbon potential, while estimates of initial source-rock distribution, thickness, and quality are key input parameters for hydrocarbon generation models. In basin models, these estimates are supplied as maps created by interpolation between observed well data and extrapolation of trends. Conceptual or simplified maps of average values are often used in frontier exploration areas where well data are sparse. In the past, much effort has been put into improving the algorithms describing the thermal evolution of basins and also improving the kinetic schemes of transformation of different assemblages of organic matter into hydrocarbons (Hantschel and Kauerauf, 2009). However, hydrocarbons expelled from a source rock are not only dependent on kerogen transformation. The spatial distribution and quality of organic matter also play an important role in determining the composition and volume of hydrocarbons available for migration (Mann and Zweigel, 2008; Tømmerås and Mann, 2008).

COMPARISON WITH ADJACENT AREAS OF THE SPB

The Polish Basin consists of the most eastern part of the SPB, extending from the UK to Poland (Van Wees et al., 2000; Maystrenko et al., 2008; Doornenbal and Stevenson, 2010). Therefore, an obvious comparison is with the North Sea Basin and adjacent areas. Recent summaries of the petroleum systems of the SPB area were published by Pletsch et al. (2010) and by Kilhams et al. (2018a). Similar Zechstein-sourced oil and gas fields are known from Poland, Germany, and from the UK in the North Sea area (e.g., Pletsch et al., 2010; Peryt et al., 2010; Reijers, 2012). Whereas, in the Mesozoic succession of the North Sea Basin and adjacent areas, the amount of organic matter deposited in the sediments is greater than in the Polish Basin. Moreover, the Mesozoic deposits of the North Sea basin experienced higher temperatures in many zones, which in turn led to a greater degree of thermal maturity of the organic matter, thus a greater transformation of the kerogen towards the generation of hydrocarbons (Cornford, 1998; Pletsch et al., 2010; Reijers, 2012). In the North Sea area, the burial history of the source rock, which was conditioned by significant subsidence in the Cenozoic, played a fundamental role in the development of hydrocarbon generation processes. Despite Late Cretaceous tectonic inversion and Paleogene erosion in some areas, the maximum palaeotemperature occurs nowadays in at least the Late Cenozoic (Cornford, 1998; Pletsch et al., 2010).

The primary source rocks in the North Sea area are mature Upper Jurassic–lowermost Cretaceous marine shales of the Farsund, Mandal, Kimmeridge Clay, Heather Formations and equivalents (Cornford, 1998; Justwan et al., 2005; Pletsch et al., 2010; Petersen et al., 2008, 2017). Deposition of these source intervals was contemporaneous with Late Jurassic synrift fault activity and their postrift subsidence, which led to thermal maturation, and petroleum generation and migration from the early Cenozoic to the present day. In the North Sea area, hydrocarbon generation has been initiated in most zones in the last several million years. It formed the developing petroleum system, where extensional fault blocks created traps containing reservoir–seal pairs that received their petroleum charge from neighbouring kitchen areas (Burley, 1993; Cornford, 1998). The main source rock of the Kimmeridge Clay Formation actively generated hydrocarbons, which then underwent intense expulsion in various zones of the North Sea Basin at temperatures >95°C and at a burial depths of >3 km (Cornford, 1998). These hydrocarbons migrated to the nearest reservoir rocks: in the northern and central part of the North Sea basin to the Jurassic sandstones (Viking graben), and in the southern part to the carbonate formations of the Upper Cretaceous. The vast majority of oil and gas fields occur in the immediate vicinity of the actively generating Kimmeridge Clay Formation (Cornford, 1998). Petroleum deposits located farther from this zone (e.g., Beatrice, Bream) show different geochemical characteristics, because their source was Devonian lacustrine mudstones and Middle Jurassic paralic coals (Peters et al., 1989; Cornford, 1998). Mid-Jurassic coals are also the source of the Harald natural gas field in the Danish sector (Pletsch et al., 2010; Petersen et al., 2008, 2017). Although the most important effective source rock in the North Sea basin is undoubtedly the Kimmeridge Clay Formation, the hydrocarbons in several reservoirs derive from other source rocks. High TOC characterizes also parts of the Lower and Middle Jurassic, Zechstein, Carboniferous, and the Middle Devonian sedimentary sequences (Cornford, 1998; Underhill and Richardson, 2022). In addition, the Upper Triassic (Raethian) of the Dutch part of the Viking graben is considered a moderately effective source rock (Clark-Lowes et al., 1987). Whereas, in the Paris

Basin, the Upper Triassic carbonate-clay deposits can also be an effective source rock (Cornford, 1998). Migration in the North Sea Basin was relatively short, limited to drainage zones of local structures (Cornford, 1998; Pletsch et al., 2010; Petersen and Hertle, 2018; Schovsbo and Jakobsen, 2019).

In the North Sea basin, Triassic deposits have mild generation potential (Cornford, 1998). However, in certain zones north of 60°N occur marine strata that show source rock characteristics. Oil and gas discoveries in the southern Barents Sea were sourced by Middle Triassic shales, which are also considered as potential oil-prone source rocks in the northern Barents Sea. The organic richness and petroleum generation potential of source rocks increase upwards from the Early to Middle Triassic. Good to excellent source rocks with dominantly type II kerogen occur in the southern Barents Sea (Steinkobbe Formation; Isaksen and Bohacs, 1995) and in east Svalbard (Botneheia Formation; Vigran et al., 2008; Krajewski, 2013). Mid-Triassic black shales of the Botneheia Formation (~80–170 m-thick) contain organic matter (3.0–5.5% TOC) of mixed oil-gas-generating type (type II/III). The degree of thermal maturity of these shales ranges from immature to the peak of the oil window (Mørk and Bjørøy 1984; Cornford, 1998; Wesenlund et al., 2021). Lower to Middle Triassic shales, which are proven source rocks on Svalbard, generated petroleum, but the timing of generation and expulsion vary considerably depending on the amount of burial (Lutz et al., 2021). Basin modelling of the Hammerfest Basin of the Barents Sea indicates that the Middle Triassic source rocks expelled petroleum as early as Early Cretaceous time, with total expelled petroleum estimated to be ~62 Gt (Rodrigues Duran et al., 2013b). Geochemical analyses of petroleum from the Goliat field support a Triassic source contribution to its Triassic reservoirs (Rodrigues Duran et al., 2013a).

These findings allow to assume that also in the Polish Basin there exist some unrecognized effective source rocks. It is impossible to distinguish a single factor that determines the lack of discovered hydrocarbon deposits in the Mesozoic strata of the Polish Basin. Although the amount of geochemical data is insufficient to draw final conclusions, it seems that in the Triassic strata in the deeply buried zones of the central part of the MPT i.e., in the Kujawy, the Mogilno–Łódź Depression and adjacent areas, the processes of generating of hydrocarbons developed in the Mesozoic. In the Zechstein Main Dolomite source rocks, hydrocarbon generation developed as (i) a single-stage process, in which full generation of hydrocarbons occurred in the Triassic; or (ii) a two-stage process, in which most hydrocarbons were generated by the end of the Jurassic, with final generation completed in the Late Cretaceous. In the remaining areas of the Polish Basin, there were not enough favourable conditions for the development of hydrocarbon generation. The main phase of hydrocarbon generation most likely occurred in the Late Triassic to the Late Jurassic. The Cretaceous strata should be excluded from potential source rocks due to insufficient thermal transformation of the organic matter. The Kimmeridgian strata, the richest in organic matter, probably did not enter the oil window in most parts of the Polish Basin (Kosakowski et al., 2015; Więclaw, 2016). The Lower-Middle Jurassic strata, predominantly contain type III organic matter which is sufficiently transformed, but has a humic character – mainly gas-forming. As a result, mainly gaseous hydrocarbons were generated, and to a lesser extent liquid (Kosakowski et al., 2015; Więclaw, 2016). In the area of the Polish Basin, the degree of kerogen transformation has remained unchanged since the end of the Cretaceous. Moreover, as a result of significant Late Cretaceous tectonic inversion, a large proportion of the hydrocarbons generated were probably destroyed. For further

analysis of a possible Mesozoic petroleum system, hydrocarbon migration routes also need to be quantified, and it is necessary to precisely define the effective source rocks that actively generated hydrocarbons before the Late Cretaceous inversion.

CONCLUSIONS

One-dimensional thermal maturity modelling has been performed assuming that heat transfer was by conduction, in steady-state thermal conditions, and the heat came from the basement but not from radiogenic heat sources within sedimentary rocks analysed. The kinetic models of hydrocarbon generation applied (Pepper and Corvi, 1995) are among the most widely used in basin modelling studies; other kinetic models would give slightly different results.

The most important results of the thermal maturity modelling can be summarized as follows: The maximum burial depth of Zechstein Main Dolomite and Upper Triassic strata reached >5 km during the Late Cretaceous. The highest kerogen transformation ratio occurred in zones of maximum thermal maturity of the organic matter. The thermogenic generation of hydrocarbons from the Zechstein Main Dolomite source rocks took place from the early Triassic throughout the Mesozoic up to the Late Cretaceous. *TR* reached different values in the

range ~10 to 100%. Hydrocarbon generation followed two stages: (i) a single-stage process, in which full generation of hydrocarbons occurred in the Triassic; and (ii) a two-stage process, in which most hydrocarbons were generated by the end of the Jurassic, with generation completed in the Late Cretaceous. The source rocks of the Upper Triassic generated hydrocarbons in the Jurassic and Cretaceous; however, most of the transformation into hydrocarbons occurred up to the Late Jurassic. *TR* in the Upper Triassic source rocks is generally lower than in the Zechstein Main Dolomite due to lesser burial. In the Upper Triassic source rocks, the highest *TR* values (>50%) were calculated along the MPT axis, in the area between the boreholes Piła IG 1 and Piotrków Trybunalski IG 1, while the most pronounced zone is in the Krośniewice Trough (i.e., Krośniewice IG 1 to Budziszewice IG 1 area), where *TR* locally reached >90%. Hydrocarbon generation continued until the Late Cretaceous, and was completed with the tectonic inversion of the Polish Basin. Changes in the burial depocentres in the central part of the basin were controlled by tectonics.

Acknowledgements. This work was supported by a statutory works subvention no. 16.16.140.315 from the AGH University of Science and Technology. Two anonymous reviewers and Dr. H. Kiersnowski are thanked for their insightful comments.

REFERENCES

- Aguilera, R., 2018.** The uncertainty in the Transformation Ratio and its impact in Oil and Gas Exploration – Part I; <https://www.linkedin.com/pulse/uncertainty-transformation-ratio-its-impact-oil-gas-roberto-aguilera/>, access on 30 December 2022
- Bachleda-Curuś, T., Semyrka, R., 1990.** The hydrocarbon balance for the Mesozoic sedimentary complex in the central part of the Polish Lowland (in Polish with English summary). Wydawnictwa AGH, Kraków.
- Bachleda-Curuś, T., Burzewski, W., Halat, Z., Semyrka, R., 1996.** Hydrocarbon generation potential of sedimentary formations in the Western Pomerania. *Oil and Gas News*, 6: 163–170.
- Bachmann, G.H., Geluk, M.C., Warrington, G., Becker-Roman, A., Beutler, G., Hagdorn, H., Hounslow, M.W., Nitsch, E., Röhling, H.-G., Simon, T., Szulc, A., 2010.** Triassic. In: *Petroleum Geological Atlas of the Southern Permian Basin Area* (eds. J.C. Doornenbal and A.G. Stevenson): 148–173. EAGE, Houten, Netherlands.
- Behar, F., Delhaye-Prat, V., Garel S., 2020.** Detrital input quantification in lacustrine petroleum systems: an example of the pre-salt source rocks from the Lower Congo Basin (Congo). *The Depositional Record*, 7: 147–171; <https://doi.org/10.1002/dep2.131>
- Bohacs, K.M., Carroll, A.R., Neal, J.E., Mankiewicz, P., 2000.** Lake-basin type, source potential, and hydrocarbon character: an integrated sequence- stratigraphic-geochemical framework. *AAPG Studies in Geology*, 46: 3–4; <https://doi.org/10.1306/St46706C1>
- Bohacs, K.M., Grabowski, G.J.J., Carroll, A.R., Mankiewicz, P.J., Miskellgerhardt, K.J., Schwalbach, J.R., Wegner, M.B., Simo, J.A., 2005.** Production, destruction, and dilution: the many paths to source-rock development. *SEPM Special Publication*, 82: 61–101.
- Botor, D., 2011.** One-dimensional modeling of gas generation processes in Carboniferous sediments from the deep part of Polish Rotliegend basin. *Geology, Geophysics and Environment*, 37: 503–516; <https://doi.org/10.7494/geol.2011.37.4.503>
- Botor, D., 2021.** Burial and thermal history modeling of the Paleozoic-Mesozoic basement in the northern margin of the Western Outer Carpathians (case study from Pilzno-40 well, Southern Poland). *Minerals*, 11: 733; <https://doi.org/10.3390/min11070733>
- Botor, D., Papiernik, B., Maćkowski, T., Reicher, B., Kosakowski, P., Machowski, G., Górecki, W., 2013.** Gas generation in Carboniferous source rocks of the Variscan Foreland Basin: implications for a charge history of Rotliegend deposits with natural gases. *Annales Societatis Geologorum Poloniae*, 83: 353–383.
- Botor, D., Anczkiewicz, A.A., Dunkl, I., Golonka, J., Paszkowski, M., Mazur, S., 2018.** Tectonothermal history of the Holy Cross Mountains (Poland) in the light of low-temperature thermochronology. *Terra Nova*, 30: 270–278; <https://doi.org/10.1111/ter.12336>
- Botor, D., Golonka, J., Anczkiewicz, A. A., Dunkl, I., Papiernik, B., Zając, J., Guzy, P., 2019a.** Burial and thermal history of the Lower Paleozoic petroleum source rocks in the SW margin of the East European Craton (Poland). *Annales Societatis Geologorum Poloniae*, 89: 31–62; <https://doi.org/10.14241/asgp.2019.12>
- Botor, D., Golonka, J., Zając, J., Papiernik, B., Guzy, P., 2019b.** Petroleum generation and expulsion in the Lower Palaeozoic petroleum source rocks at the SW margin of the East European Craton (Poland). *Annales Societatis Geologorum Poloniae*, 89: 63–89; <https://doi.org/10.14241/asgp.2019.11>
- Botor, D., Mazur, S., Anczkiewicz, A.A., Dunkl, I., Golonka, J., 2021.** Thermal history of the East European Platform margin in Poland based on apatite and zircon low-temperature thermochronology. *Solid Earth*, 12: 1899–1930; <https://doi.org/10.5194/se-12-1899-2021>
- Burley, S.D., 1993.** Models of burial diagenesis for deep exploration in Jurassic fault traps of the Central and Northern North Sea. *Petroleum Geology Conference Series*, 4: 1353–1375; <https://doi.org/10.1144/0041353>

- Burnham, A.K., Peters, K.E., Schenk, O., 2016.** Evolution of vitrinite reflectance models. In: AAPG Annual Convention and Exhibition, Calgary, Alberta Canada, June 19–22, 2016.
- Clark-Lowes, D.D., Kuzemko, N.C.J., Scott, D.A., 1987.** Structure and petroleum prospectivity of the Dutch Central Graben and neighbouring platform areas. In: Proc. 3rd Conf. on Petroleum Geology of NW Europe (eds. J. Brooks and K.W. Glennie): 337–356. Graham & Trotman, London.
- Cornford, C., 1998.** Source rocks and hydrocarbons of the North Sea. In: Petroleum geology of the North Sea: basic concepts and recent advances (ed. K.W. Glennie): 376–462. 4th ed., Oxford, United Kingdom, Blackwell Science Ltd.
- Dadlez, R., 2006.** The Polish Basin-relationship between the crystalline, consolidated and sedimentary crust. *Geological Quarterly*, **50** (1): 43–58.
- Dadlez, R., Narkiewicz, M., Stephenson, R.A., Visser, M.T.M., Van Wees, J.D., 1995.** Tectonic evolution of the Mid-Polish Trough: modelling implications and significance for central European geology. *Tectonophysics*, **252**: 179–195; [https://doi.org/10.1016/0040-1951\(95\)00104-2](https://doi.org/10.1016/0040-1951(95)00104-2)
- Dadlez, R., Marek, S., Pokorski, J., 1998.** Paleogeographical Atlas of the Epicontinental Permian and Mesozoic of Poland. Państwowy Instytut Geologiczny, Warszawa.
- Do Couto, D., Garel, S., Moscardiello, A., Bou Daher, S., Littke, R., Weniger, P., 2021.** Origins of hydrocarbons in the Geneva Basin: insights from oil, gas and source rock organic geochemistry. *Swiss Journal of Geosciences*, **114**, 11; <https://doi.org/10.1186/s00015-021-00388-4>
- Doornenbal, J.C., Stevenson, A.G. (eds), 2010.** Petroleum Geological Atlas of the Southern Permian Basin Area. EAGE, Houten, Netherlands.
- Doornenbal, J.C., Kombrink, H., Bouroullac, R., Dalman, R.A.F., De Bruin, G., Geel, C. R., Houben, A.J.P., Jaarsma, B., Juez-Larré, J., Kortekaas, M., Mijnlieff, H.F., Nelskamp, S., Pharaoh, T.C., Ten Veen, J. H., Ter Borgh, M., Van Ojik, K., Verreussel, R.M.C.H., Verweij, J.M., Vis, G.J., 2019.** New insights on subsurface energy resources in the Southern North Sea Basin area. *Geological Society, Special Publications*, **494**: 233–268; <https://doi.org/10.1144/SP494-2018-178>
- Dyrka, I. (ed.), 2017.** Ocena perspektywiczności geologicznej zasobów złóż węglowodorów oraz przygotowanie materiałów na potrzeby przeprowadzenia postępowania przetargowego w celu udzielenia koncesji na poszukiwanie i rozpoznawanie lub wydobywanie złóż węglowodorów Zadanie 22.5004.1502.02.0. Pakiet danych geologicznych dla postępowania przetargowego na poszukiwanie złóż węglowodorów Obszar przetargowy "Szamotyły – Poznań Północ" (in Polish). PIG Warszawa web data base, access on 11 January 2022.
- Eisbacher, G.H., Fielitz, W., 2010.** Karlsruhe und seine Region. Sammlung Geologischer Führer, **103**. Borntraeger, Stuttgart.
- Feist-Burkhardt, S., Götz, A.E., Szulc, J., Aigner, T., Borkhataria, R., Geluk, M., Haas, J., Hornung, J., Jordan, P., Kempf, O., Michalík, J., Nawrocki, J., Reinhardt, L., Ricken, W., Röhling, H.G., Ruffer, T., Török, A., Zuhlke, R., 2008.** Triassic. In: *The Geology of Central Europe* (ed. T. McCann): 749–821. The Geological Society, London.
- Geluk, M., Mckie T., Kilhams, B., 2018.** An introduction to the Triassic: current insights into the regional setting and energy resource potential of NW Europe. *Geological Society Special Publications*, **469**: 139–147; <https://doi.org/10.1144/SP469.1>
- Geršlová, E., Opletal, V., Sýkorová, I., Sedláková, I., Geršl, M., 2015.** A geochemical and petrographical characterization of organic matter in the Jurassic Mikulov Marls from the Czech Republic. *International Journal of Coal Geology*, **141–142**: 42–50; <https://doi.org/10.1016/j.coal.2015.03.002>
- Grotek, I., 1998.** Thermal maturity of organic matter in the Zechstein deposits of the Polish Lowlands area (in Polish with English summary). *Prace Państwowego Instytutu Geologicznego*, **165**: 255–259.
- Grotek, I., 2006.** Thermal maturity of organic matter from the sedimentary cover deposits from Pomeranian part of the TESZ, Baltic Basin and adjacent area (in Polish with English summary). *Prace Państwowego Instytutu Geologicznego*, **186**: 253–270.
- Hantschel, T., Kauerauf, A.I., 2009.** Fundamentals of basin and petroleum systems modelling. Springer, Heidelberg.
- Hunt, J.M., 1996.** *Petroleum Geochemistry and Geology*, 2nd Edition. W.H. Freeman and Company.
- Isaksen, G.H., Bohacs, K.M., 1995.** Geological controls of source rock geochemistry through relative sea level; Triassic, Barents Sea. In: *Petroleum Source Rocks* (ed. B.J. Katz): 25–50. Springer Berlin Heidelberg, Berlin, Heidelberg.
- Justwan, H., Dahl, B., Isaksen, G.H., Meisingset, I., 2005.** Late and Middle Jurassic source facies and quality variations, South Viking Graben, North Sea. *Journal of Petroleum Geology*, **28**: 241–268; <https://doi.org/10.1111/j.1747-5457.2005.tb00082.x>
- Karnkowski, P.H., 1996.** Thermal history and hydrocarbon generation in the area of Dobrzyca structure, Western Pomerania, Poland (in Polish with English summary). *Przegląd Geologiczny*, **44**: 349–357.
- Karnkowski, P.H., 1999a.** Oil and Gas Deposits in Poland. Geological Society "Geos", Kraków.
- Karnkowski, P.H., 1999b.** Origin and evolution of the Polish Rotliegend Basin. *Polish Geological Institute Special Papers*, **3**: 1–93.
- Karnkowski, P.H., 2007a.** Permian basin as a main exploration target in Poland. *Przegląd Geologiczny*, **55**: 1003–1015.
- Karnkowski, P.H., 2007b.** Petroleum provinces in Poland. *Przegląd Geologiczny*, **55**: 1061–1067.
- Katz, B.J., 2005.** Controlling factors on source rock development—a review of productivity, preservation, and sedimentation rate. *SEPM, Special Publication*, **82**: 7–16.
- Katz, B., Lin, F., 2014.** Lacustrine basin unconventional resource plays: key differences. *Marine and Petroleum Geology*, **56**: 255–265; <https://doi.org/10.1016/j.marpetgeo.2014.02.013>
- Kiersnowski, H., 2013.** Late Permian aeolian sand seas from the Polish Upper Rotliegend Basin in the context of palaeoclimatic periodicity. *Geological Society Special Publications*, **376**: 431–456; <http://dx.doi.org/10.1144/SP376.20>
- Kiersnowski, H., (ed.) 2017.** Ocena perspektywiczności geologicznej zasobów złóż węglowodorów oraz przygotowanie materiałów na potrzeby przeprowadzenia postępowania przetargowego w celu udzielenia koncesji na poszukiwanie i rozpoznawanie lub wydobywanie złóż węglowodorów – etap II. Zadanie no 22.5004.1502.08.0. Pakiet danych geologicznych do postępowania przetargowego na poszukiwanie złóż węglowodorów Obszar przetargowy "Piła" (in Polish). PIG Warszawa web data base, access on 10 January 2022.
- Kiersnowski, H., Tomaszczyk, M., 2010.** Permian dune fields as geomorphic traps for gas accumulation: Upper Rotliegend-Zechstein Basin, SW Poland. In: 18th International Sedimentological Congress Abstracts Volume, Mendoza (eds. E. Schwarz, S. Georgieff, E. Piovano and D. Ariztegui): 944.
- Kiersnowski, H., Paul, J., Peryt, T.M., Smith, D.B., 1995.** Facies, paleogeography and sedimentary history of the Southern Permian Basin in Europe. In: *The Permian of Northern Pangea – Sedimentary Basins and Economic Resources* (eds. P.A. Scholle, T.M. Peryt and D.S. Ulmer-Scholle): 119–136. Springer-Verlag, Berlin.
- Kiersnowski, H., Buniak, A., Kuberska, M., Srokowska-Okońska, A., 2010.** Tight gas accumulations in Rotliegend sandstones of Poland (in Polish with English summary). *Przegląd Geologiczny*, **58**: 335–346.
- Kilhams, B., Kukla, P.A., Mazur, S., Mckie, T., Mijnlieff, H.F. Van Ojik, K., Rosendaal, E., 2018a.** Mesozoic resource potential in the Southern Permian Basin area: the geological key to exploiting remaining hydrocarbons whilst unlocking geothermal potential. *Geological Society Special Publications*, **469**: 1–18; <https://doi.org/10.1144/SP469.26>
- Kilhams, B., Stevanovic, S., Nicolai, C., 2018b.** The 'Buntsandstein' gas play of the Horn Graben (German, Danish offshore): dry well analysis, remaining hydrocarbon potential. *Geological Society Special Publications*, **469**: 19–28; <https://doi.org/10.1144/SP469.5>

- Kortekaas, M., Böker, U., Van Der Kooij, C., Jaarsma, B., 2018.** Lower Triassic reservoir development in the Dutch northern offshore. *Geological Society Special Publications*, **469**: 56–77; <https://doi.org/10.1144/SP469.19>
- Kosakowski, P., Krajewski, M., 2014.** Hydrocarbon potential of the Zechstein Main Dolomite in the western part of the Wielkopolska platform, SW Poland: new sedimentological and geochemical data. *Marine and Petroleum Geology*, **49**: 99–120; <https://doi.org/10.1016/j.marpetgeo.2013.10.002>
- Kosakowski, P., Krajewski, M., 2015.** Hydrocarbon potential of the Zechstein Main Dolomite (Upper Permian) in western Poland: relation to organic matter and facies characteristics. *Marine and Petroleum Geology*, **68**: 675–694; <https://doi.org/10.1016/j.marpetgeo.2015.03.026>
- Kosakowski, P., Wróbel, M., Poprawa, P., 2010.** Hydrocarbon generation and expulsion modelling of the lower Paleozoic source rocks in the Polish part of the Baltic region. *Geological Quarterly*, **54** (2): 241–256.
- Kosakowski, P., Wójcik-Tabol, P., Kowalski, A., Zacharski, J., 2015.** Jurassic petroleum system in the Polish Lowlands (central Poland) – organic geochemical and numerical modelling approach. 77th EAGE Conference and Exhibition 2015 Madrid, Spain, 1–4 June 2015, W P7 02: 1–6.
- Kotarba, M., Wagner, R., 2007.** Generation potential of the Zechstein Main Dolomite (Ca2) carbonates in the Gorzów Wielkopolski-Międzychód-Lubiatów area: geological and geochemical approach to microbial-algal source rock. *Przegląd Geologiczny*, **55**: 1025–1036.
- Kotarba, M.J., Pokorski, J., Grzelowski, C., Kosakowski, P., 2005.** Origin of natural gases accumulated in Carboniferous and Rotliegend strata on the Baltic part of the Western Pomerania (in Polish with English summary). *Przegląd Geologiczny*, **53**: 425–433.
- Kotarba, M.J., Peryt, T.M., Kosakowski, P., Więclaw, D., 2006.** Organic geochemistry, depositional history and hydrocarbon generation modelling of the Upper Permian Kupferschiefer and Zechstein Limestone strata in south-west Poland. *Marine and Petroleum Geology*, **23**: 371–386; <http://dx.doi.org/10.1016/j.marpetgeo.2005.10.003>
- Kotarba, M.J., Więclaw, D., Bilkiewicz, E., Dziadzio, P., Kowalski, A., 2017a.** Genetic correlation of source rocks and natural gas in the Polish Outer Carpathians and Paleozoic-Mesozoic basement east of Kraków (Southern Poland). *Geological Quarterly*, **61** (4): 795–824; <https://doi.org/10.7306/gq.1367>
- Kotarba, M.J., Bilkiewicz, E., Hałas, S., 2017b.** Mechanisms of generation of hydrogen sulphide, carbon dioxide and hydrocarbon gases from selected petroleum fields of the Zechstein Main Dolomite carbonates of the western part of Polish Southern Permian Basin: Isotopic and geological approach. *Journal of Petroleum Science and Engineering*, **157**: 380–391; <https://doi.org/10.1016/j.petrol.2017.07.015>
- Kotarba, M.J., Bilkiewicz, E., Kosakowski, P., 2020.** Origin of hydrocarbon and non-hydrocarbon (H₂S, CO₂ and N₂) components of natural gas accumulated in the Zechstein Main Dolomite carbonate reservoir of the western part of the Polish sector of the Southern Permian Basin. *Chemical Geology*, **554**: 119807; <https://doi.org/10.1016/j.chemgeo.2020.119807>
- Kovalevych, V.M., Peryt, T.M., Shanina, S.N., Więclaw, D., Lytvyniuk, S.F., 2008.** Geochemical aureoles around oil and gas accumulations in the Zechstein (Upper Permian) of Poland: Analysis of fluid inclusions in halite and bitumens in salt. *Journal of Petroleum Geology*, **31**: 245–262; <http://dx.doi.org/10.1111/j.1747-5457.2008.00419.x>
- Kowalska, S., Wójtowicz, A., Hałas, S., Wemmer, K., Mikołajewski, Z., Buniak, A., 2019.** Thermal history of Lower Palaeozoic rocks from the East European Platform margin of Poland based on K-Ar age dating and illite-smectite palaeothermometry. *Annales Societatis Geologorum Poloniae*, **89**: 481–509; <https://doi.org/10.14241/asgp.2019.21>
- Kozłowska, A., Poprawa, P., 2004.** Diagenesis of the Carboniferous clastic sediments of the Mazowsze region and the northern Lublin region related to their burial and thermal history (in Polish with English summary). *Przegląd Geologiczny*, **52**: 491–500.
- Krajewski, K.P., 2013.** Organic matter-apatite-pyrite relationships in the Botneheia Formation (Middle Triassic) of eastern Svalbard: relevance to the formation of petroleum source rocks in the NW Barents Sea shelf. *Marine and Petroleum Geology*, **45**: 69–105; <https://doi.org/10.1016/j.marpetgeo.2013.04.016>
- Kuberska, M., Kiersnowski, H., Poprawa, P., Kozłowska, A., 2021.** Rotliegend sedimentary rocks in the Kutno 2 well under conditions of a postulated Jurassic thermal event and high overpressure - a petrographic study (in Polish with English summary). *Przegląd Geologiczny*, **69**: 365–373; <https://doi.org/10.7306/2021.19>
- Kus, J., Cramer, B., Kockel, F., 2005.** Effects of a Cretaceous structural inversion and a postulated high heat flow event on petroleum system of the western Lower Saxony Basin and the charge history of the Apeldorn gas field. *Geologie en Mijnbouw*, **84**: 3–24; <https://doi.org/10.1017/S0016774600022873>
- Krzywiec, P., 2002.** Mid-Polish Trough inversion - seismic examples, main mechanisms and its relationship to the Alpine-Carpathian collision. *European Geosciences Union, Stephan Mueller Special Publication Series*, **1**: 151–165.
- Krzywiec, P., 2004.** Triassic evolution of the Kłodawa salt structure: Basement-controlled salt tectonics within the Mid-Polish Trough (central Poland). *Geological Quarterly*, **48** (2): 123–134.
- Krzywiec, P., 2006a.** Triassic-Jurassic evolution of the Pomeranian segment of the Mid-Polish Trough – basement tectonics and sedimentary patterns. *Geological Quarterly*, **50** (1): 139–150.
- Krzywiec, P., 2006b.** Structural inversion of the Pomeranian and Kuiavian segments of the Mid-Polish Trough – lateral variations in timing and structural style. *Geological Quarterly*, **50** (1): 151–168.
- Krzywiec, P., 2009.** Devonian-Cretaceous repeated subsidence and uplift along the Teisseyre-Tornquist zone in SE Poland – insight from seismic data interpretation. *Tectonophysics*, **475**: 142–159; <https://doi.org/10.1016/j.tecto.2008.11.020>
- Krzywiec, P., Peryt, T.M., Kiersnowski, H., Pomianowski, P., Czapowski, G., Kwolek K., 2017a.** Permo-Triassic evaporites of the Polish Basin and their bearing on the tectonic evolution and hydrocarbon system, an Overview. In: *Permo-Triassic Salt Provinces of Europe, North Africa and the Atlantic Margins* (eds. J.I. Soto, J.F. Flinch and G. Tari): 243–261; <https://doi.org/10.1016/B978-0-12-809417-4.00012-4>
- Krzywiec, P., Gągała, Ł., Mazur, S., Słonka, Ł., Kufraś, M., Malinowski, M., Pietsch, K., Golonka, J., 2017b.** Variscan deformation along the Teisseyre-Tornquist Zone in SE Poland: thick-skinned structural inheritance or thin-skinned thrusting? *Tectonophysics*, **718**: 83–91; <https://doi.org/10.1016/j.tecto.2017.06.008>
- Krzywiec, P., Stachowska, A., Stypa, A., 2018.** The only way is up – on Mesozoic uplifts and basin inversion events in SE Poland. *Geological Society Special Publications*, **469**: 33–57; <https://doi.org/10.1144/SP469.14>
- Kutek, J., 1994.** Jurassic tectonic events in south-eastern cratonic Poland. *Acta Geologica Polonica*, **44**: 167–221.
- Kutek, J., 2001.** The Polish-Mesozoic rift basin. *Memoirs du Muséum National d'Histoire Naturelle*, **186**: 213–236.
- Kutek, J., Głazek, J., 1972.** The Holy Cross area, central Poland, in the Alpine cycle. *Acta Geologica Polonica*, **22**: 603–653.
- Labus, K., Tarkowski, R., 2022.** Modeling hydrogen-rock-brine interactions for the Jurassic reservoir and cap rocks from Polish Lowlands. *International Journal of Hydrogen Energy*, **47**: 10947–10962; <https://doi.org/10.1016/j.ijhydene.2022.01.134>
- Labus, K., Tarkowski, R., Wdowin, M., 2014.** Modeling gas-rock-water interactions in carbon dioxide storage capacity assessment: A case study of Jurassic sandstones in Poland. *International Journal of Environmental Science and Technology*, **12**: 2493–2502; <https://doi.org/10.1007/s13762-014-0652-6>
- Lamarche, J., Scheck, M., Lewerenz, B., 2003.** Heterogeneous tectonic inversion of the Mid-Polish Trough related to crustal architecture, sedimentary patterns and structural inheritance. *Tectonophysics*, **373**: 75–92; [https://doi.org/10.1016/S0040-1951\(03\)00285-3](https://doi.org/10.1016/S0040-1951(03)00285-3)

- Lutz, M., Cleintuar, M., 1999.** Geological results of a hydrocarbon exploration campaign in the southern Upper Rhine Graben. *Bulletin for Applied Geology*, **4**: 3–80.
- Lutz, R., Klitzke, P., Weniger, P., Blumenberg, M., Franke, D., Lutz, R., Ehrhardt, W., Berglar, K., 2021.** Basin and petroleum systems modelling in the northern Norwegian Barents Sea. *Marine and Petroleum Geology*, **130**: 105128; <https://doi.org/10.1016/j.marpetgeo.2021.105128>
- Łuszczak, K., Wyglądała, M., Śmigieński, M., Waliczek, M., Matyja, B.A., Konon, A., Ludwiniak, M., 2020.** How to deal with missing overburden – investigating Late Cretaceous exhumation of the Mid-Polish anticlinorium by a multi-proxy approach. *Marine and Petroleum Geology*, **114**: 104229; <https://doi.org/10.1016/j.marpetgeo.2020.104229>
- Maćkowski, T., 2005.** Wpływ dolnopermijskiego wulkanizmu na stopień przeobrażenia termicznego karbońskich skał macierzystych na obszarze monokliny przedsudeckiej (in Polish). In: *Sprawozdania z Seminariów Naukowych AGH ZSE* (ed. J. Kuśmierk): 120–122, Kraków.
- Majorowicz, J., 2021.** Review of the heat flow mapping in Polish sedimentary basin across different tectonic terrains. *Energies*, **14**: 6103; <https://doi.org/10.3390/en14196103>
- Majorowicz, J., Wybraniec, S., 2011.** New terrestrial heat flow map of Europe after regional paleoclimatic correction application. *International Journal of Earth Sciences*, **100**: 881–887; <https://doi.org/10.1007/s00531-010-0526-1>
- Majorowicz, J.A., Marek S., Znosko J., 1984.** Paleogeothermal gradients by vitrinite reflectance data and their relation to the present geothermal gradient patterns of the Polish Lowland. *Tectonophysics*, **103**: 141–156; [https://doi.org/10.1016/0040-1951\(84\)90079-9](https://doi.org/10.1016/0040-1951(84)90079-9)
- Mann, U., Zweigel, J., 2008.** Modeling source rock distribution and quality variations: the OF-Mod approach. *IAS Special Publication*, **40**: 239–274.
- Marek S., Znosko J., 1972.** Tectonics of the Kujawy Region (in Polish with English summary). *Kwartalnik Geologiczny*, **16** (1): 1–18.
- Marek, S., Pajchłowa, M., (eds.), 1997.** Epikontynentalny perm i mezozoik w Polsce (in Polish). *Prace Państwowego Instytutu Geologicznego*, **153**: 1–284.
- Marynowski, L., Simoneit, B.R.T., 2009.** Widespread Upper Triassic–Lower Jurassic wildfire records from Poland: evidence from charcoal and pyrolytic polycyclic aromatic hydrocarbons. *Palaios*, **24**: 785–798; <https://www.jstor.org/stable/40606423>
- Marynowski, L., Wyszomirski, P., Kurkiewicz, S., 2006.** The characteristics of organic matter from the Triassic clays of NW margin of the Holy Cross Mts. (Poland) – preliminary report. *Mineralogia*, **37**: 113–122; <https://doi.org/10.2478/v10002-007-0003-z>
- Maystrenko, Y., Bayer, U., Brink, H.J., Littke, R., 2008.** The Central European Basin System – an overview. In: *Dynamics of Complex Intracontinental Basins: The Central European Basin System* (eds. R. Littke, U. Bayer, D. Gajewski and S. Nelskamp): 15–34. Springer, Berlin.
- Mazur, S., Scheck-Wenderoth, M., Krzywiec, P., 2005.** Different modes of the late Cretaceous–early Tertiary inversion in the north German and Polish Basins. *International Journal of Earth Sciences*, **94**: 782–798; <https://doi.org/10.1007/s00531-005-0016-z>
- Mazur, S., Aleksandrowski, P., Kryza, R., Oberc-Dziedzic, T., 2006.** The Variscan Orogen in Poland. *Geological Quarterly*, **50** (1): 89–111.
- Mazur, S., Malinowski, M., Maystrenko, Y.P., Gągała, Ł., 2021.** Pre-existing lithospheric weak zone and its impact on continental rifting - The Mid-Polish Trough, Central European Basin System. *Global and Planetary Change*, **198**: 103417; <https://doi.org/10.1016/j.gloplacha.2021.103417>
- Mikołajewski, Z., Grelowski, C., Kwolek, K., Czechowski, F., Słowakiewicz, M., Matyasik, I., Grotek, I., 2019.** Hydrocarbon habitat in the Zielin Late Permian isolated carbonate platform, western Poland. *Facies*, **65**: 215–225; <https://doi.org/10.1007/s10347-018-0544-1>
- Mørk, A., Bjørøy, M., 1984.** Mesozoic source rocks on Svalbard. In: *Petroleum Geology of the North European Margin* (ed. A.M. Spencer): 371–382. Norwegian Petroleum Society/Graham & Trotman, London.
- Nemčok, M., Henk, A., 2006.** Oil reservoirs in foreland basins charged by thrustbelt source rocks: insights from numerical stress modeling and geometric balancing in the West Carpathians. *Geological Society Special Publications*, **253**: 415–428; <https://doi.org/10.1144/GSL.SP.2006.253.01.22>
- Nielsen, L.H., 2003.** Late Triassic–Jurassic development of the Danish Basin and the Fennoscandian Border Zone, southern Scandinavia. *Geological Survey of Denmark and Greenland Bulletin*, **1**: 459–526.
- Ogg, J.G., Ogg, G., Gradstein, F.M., 2008.** *The Concise Geologic Time Scale*. Cambridge University Press, Cambridge.
- Papiernik, B., Botor, D., Golonka, J., Porębski, S.J., 2019.** Unconventional hydrocarbon prospects in Ordovician and Silurian mudrocks of the East European Craton (Poland): insight from three-dimensional modelling of total organic carbon and thermal maturity. *Annales Societatis Geologorum Poloniae*, **89**: 511–533; <https://doi.org/10.14241/asgp.2019.26>
- Pepper, A.S., Corvi, P.J., 1995.** Simple kinetic models of petroleum formation. Part III: modelling an open system. *Marine and Petroleum Geology*, **12**: 417–452; [https://doi.org/10.1016/0264-8172\(95\)96904-5](https://doi.org/10.1016/0264-8172(95)96904-5)
- Peryt, T.M., Peryt, D., 2021.** Foraminiferal micro-buildups ("reefs") in the Wuchiapingian basin facies of the basal Zechstein carbonates in western Poland. *Journal of Palaeogeography*, **10**: 463–481; <https://doi.org/10.1016/j.jop.2021.08.001>
- Peryt, T.M., Geluk, M.C., Mathiesen, A., Paul, J., Smith, K., 2010.** Zechstein. In: *Petroleum Geological Atlas of the Southern Permian Basin Area* (eds. J.C. Doornenbal and A.G. Stevenson): 123–147. EAGE Publications, Houston.
- Peters, K.E., Moldowan, J.M., Driscoll, A.R., Demaison, G.J., 1989.** Origin of Beatrice oil-field by co-sourcing from Devonian and Middle Jurassic Source Rocks, Inner Moray Firth, United Kingdom. *AAPG Bulletin*, **73**: 454–471; <https://doi.org/10.1306/44B49FCE-170A-11D7-8645000102C1865D>
- Petersen, H.I., Hertle, M., 2018.** Review of the coaly source rocks and generated petroleum in the Danish North Sea: an underexplored Middle Jurassic petroleum system? *Journal of Petroleum Geology*, **41**: 135–154; <https://doi.org/10.1111/jpg.12697>
- Petersen, H.I., Nytoft, H.P., Nielsen, L.H., 2004.** Characterisation of oil and potential source rocks in the northeastern Song Hong Basin, Vietnam: indications of a lacustrine-coal sourced petroleum system. *Organic Geochemistry*, **35**: 493–515; <https://doi.org/10.1016/j.orggeochem.2004.01.011>
- Petersen, H.I., Nielsen, L.H., Bojesen-Koefoed, J.A., Mathiesen, A., Kristensen, L., Dalhoff, F., 2008.** Evaluation of the quality, thermal maturity and distribution of potential source rocks in the Danish part of the Norwegian-Danish Basin. *Geological Survey of Denmark and Greenland Bulletin*, **16**.
- Petersen, H.I., Hertle, M., Sulsbrück, H., 2017.** Upper Jurassic–lowermost Cretaceous marine shale source rocks (Farsund Formation), North Sea: kerogen composition and quality and the adverse effect of oil-based mud contamination on organic geochemical analyses. *International Journal of Coal Geology*, **173**: 26–39; <https://doi.org/10.1016/j.coal.2017.02.006>
- Pieńkowski, G., Hesselbo, S.P., Barbacka, M., Leng, M.L., 2020.** Non-marine carbon-isotope stratigraphy of the Triassic–Jurassic transition in the Polish Basin and its relationships to organic carbon preservation, pCO₂ and palaeotemperature. *Earth-Science Reviews*, **210**, 103383; <https://doi.org/10.1016/j.earscirev.2020.103383>
- Piwocki, M., 2004.** Paleogen. In: *Budowa geologiczna Polski Tom I, Stratygrafia, cz. 3a, Kenozoik, Paleogen i Neogen* (eds. T. Peryt and M. Piwocki): 22–71. Państwowy Instytut Geologiczny.
- Pletsch, T., Appel, J., Botor, D., Clayton, C.J., Duin, E.J.T., Faber, E., Górecki, W., Kombrink, H., Kosakowski, P., Kuper, G., Kus, J., Lutz, R., Mathiesen, A., Ostertag-Henning, C.,**

- Papiernik, B., Van Bergen, F., 2010.** Petroleum Generation and Migration. In: Petroleum Geological Atlas of the Southern Permian Basin Area (eds. J.C. Doornenbal and A.G. Stevenson): 225–253. EAGE Publications, Houten.
- Poprawa, P., Grotek, I., 2004.** Thermal evolution of the Permian-Mesozoic Polish Basin – model predictions confronted with analytical data. *Bollettino di Geofisica, teorica ed applicata*, **45**: 258–261.
- Poprawa, P., Andriessen, P., 2006.** Wstępne wyniki termochronologii trawowej na apatykach dla północnej i centralnej części basenu polskiego (in Polish). *Prace Państwowego Instytutu Geologicznego*, **186**: 271–292.
- Poprawa, P., Kiersnowski, H., 2008.** Potential for shale gas and tight gas exploration in Poland (in Polish with English summary). *Biuletyn Państwowego Instytutu Geologicznego*, **429**: 145–152.
- Poprawa, P., Kiersnowski, H., 2010.** Tight gas reservoirs in Poland. (In Polish with English summary). *Biuletyn Państwowego Instytutu Geologicznego*, **439**: 173–180.
- Poprawa, P., Grotek, I., Żywiecki, M.M., 2005.** Impact of the Permian magmatic activity on the thermal maturation of the Carboniferous sediments in the outer Variscan orogen (SW Poland). *Mineralogical Society of Poland, Special Papers*, **26**: 253–259.
- Powell, T.G., 1986.** Petroleum geochemistry and depositional setting of lacustrine source rocks. *Marine and Petroleum Geology*, **3**: 200–219.
- Požaryski, W., Brochwicz-Lewiński, W., 1978.** On the Polish Trough. *Geologie en Mijnbouw*, **57**: 545–557.
- Reijers, T.J.A., 2012.** Sedimentology and diagenesis as 'hydrocarbon exploration tools' in the Late Permian Zechstein-2 Carbonate Member (NE Netherlands). *Geologos*, **18**: 163–195; <https://doi.org/10.2478/v10118-012-0009-x>
- Reinhardt, L., Ricken, W., 2000.** The stratigraphic and geochemical record of playa cycles: monitoring a Pangaeen monsoon-like system (Triassic, Middle Keuper, Germany). *Palaeogeography, Palaeoclimatology, Palaeoecology*, **161**: 205–227; [https://doi.org/10.1016/S0031-0182\(00\)00124-3](https://doi.org/10.1016/S0031-0182(00)00124-3)
- Resak, M., Narkiewicz, M., Littke, R., 2008.** New basin modelling results from the Polish part of the Central European Basin system (Pomerania): implications for the Late Cretaceous-Early Paleogene structural inversion. *International Journal of Earth Sciences*, **97**: 955–972; <https://doi.org/10.1007/s00531-007-0246-3>
- Resak, M., Glasmacher, U.A., Narkiewicz, M., Littke, R., 2010.** Maturity modelling integrated with apatite fission-track dating: implications for the thermal history of the Mid-Polish Trough (Poland). *Marine and Petroleum Geology*, **27**: 108–115; <https://doi.org/10.1016/j.marpetgeo.2009.06.002>
- Rodrigues Duran, E., di Primio, R., Anka, Z., Stoddart, D., Horsfield, B., 2013a.** Petroleum system analysis of the Hammerfest Basin (southwestern Barents Sea): comparison of basin modelling and geochemical data. *Organic Geochemistry*, **63**: 105–121; <https://doi.org/10.1016/j.orggeochem.2013.07.011>
- Rodrigues Duran, E., di Primio, R., Anka, Z., Stoddart, D., Horsfield, B., 2013b.** 3D-basin modelling of the Hammerfest Basin (southwestern Barents Sea): a quantitative assessment of petroleum generation, migration and leakage. *Marine and Petroleum Geology*, **45**: 281–303; <https://doi.org/10.1016/j.marpetgeo.2013.04.023>
- Rowan, M., Krzywiec, P., 2014.** The Szamotuły salt diapir and Mid-Polish Trough: Decoupling during both Triassic-Jurassic rifting and Alpine inversion. *Interpretation*, **2**: SM1–SM18; <https://doi.org/10.1190/INT-2014-0028.1>
- Schad, A., 1962.** Voraussetzungen für die Bildung von Erdöllagerstätten im Rheingraben. *Abhandlungen des Geologischen Landesamt Baden-Württemberg*, **4**: 29–40.
- Scheck-Wenderoth, M., Lamarche, J., 2005.** Crustal memory and basin evolution in the Central European Basin System – new insights from a 3D structural model. *Tectonophysics*, **397**: 143–165; <https://doi.org/10.1016/j.tecto.2004.10.007>
- Scheck-Wenderoth, M., Krzywiec, P., Zülke, R., Maystrenko, Y., Frizheim, N., 2008.** Permian to Cretaceous tectonics. In: *The Geology of Central Europe, part 2, Mesozoic and Cenozoic* (ed. T. McCann): 999–1030. Geological Society of London, London.
- Schito, A., Andreucci, B., Aldega, L., Corrado, S., Di Paolo, L., Zattin, M., Szaniawski, R., Jankowski, L., Mazzoli, S., 2018.** Burial and exhumation of the western border of the Ukrainian Shield (Podolia): a multi-disciplinary approach. *Basin Research*, **30**: 532–549; <https://doi.org/10.1111/bre.12235>
- Schobben, M., Gravendyck, J., Mangels, F., Struck, U., Bussert, R., Kürschner, W.M., Korn, D., Sander, P.M., Aberhan, M., 2019.** A comparative study of total organic carbon-¹³C signatures in the Triassic–Jurassic transitional beds of the Central European Basin and western Tethys shelf seas. *Newsletters on Stratigraphy*, **52**: 461–486; <https://doi.org/10.1127/nos/2019/0499>
- Schovsbo, N.H., Jakobsen, F., 2019.** Review of hydrocarbon potential in East Denmark following 30 years of exploration activities. *GEUS Bulletin*, **43**, 2019430105; <https://doi.org/10.34194/GEUSB-201943-01-05>
- Słowakiewicz, M., Mikołajewski, Z., 2011.** Upper Permian Main Dolomite microbial carbonates as potential source rocks for hydrocarbons (W Poland). *Marine and Petroleum Geology*, **28**: 1572–1591; <https://doi.org/10.1016/j.marpetgeo.2011.04.002>
- Słowakiewicz, M., Blumenberg, M., Więclaw, D., Röhling, H.-G., Scheeder, G., Hindenberg, K., Leśniak, A., Idiz, E.F., Tucker, M.E., Pancost, R.D., Kotarba, M.J., Gerling, J.P., 2018.** Zechstein Main Dolomite oil characteristics in the Southern Permian Basin: I. Polish and German sectors panel. *Marine and Petroleum Geology*, **93**: 356–375; <https://doi.org/10.1016/j.marpetgeo.2018.03.023>
- Sowiżdżał, A., Semyrka, R., 2016.** Analyses of permeability and porosity of sedimentary rocks in terms of unconventional geothermal resource explorations in Poland. *Geologos*, **22**: 149–163; <https://doi.org/10.1515/logos-2016-0015>
- Sowiżdżał, A., Papiernik, B., Machowski, G., Hajto, M., 2013.** Characterization of petrophysical parameters of the Lower Triassic deposits in a prospective location for enhanced geothermal system (central Poland). *Geological Quarterly*, **57** (4): 729–744; <https://doi.org/10.7306/gq.1121>
- Stephenson, R. A., Narkiewicz, M., Dadlez, R., Van Wees, J.D., Andriessen, P., 2003.** Tectonic subsidence modelling of the Polish Basin in the light of new data on crustal structure and magnitude of inversion. *Sedimentary Geology*, **156**: 59–70; <https://doi.org/10.1016/j.sedgeo.2013.10.008>
- Sweeney, J.J., Burnham, A.K., 1990.** Evaluation of a simple model of vitrinite reflectance (EASY%R_o) based on chemical kinetics. *AAPG Bulletin*, **74**: 1559–1570; <https://doi.org/10.1306/OC9B251F-1710-11D7-8645000102C1865D>
- Szulc, J., 2000.** Middle Triassic evolution of the northern Peri-Tethys area as influenced by early opening of the Tethys ocean. *Annales Societatis Geologorum Poloniae*, **70**: 1–48.
- Szulc, J., 2007.** Chronological outline of evolution of the eastern Germanic Basin in late Ladinian - Rhaetian times. *International Workshop on the Triassic of southern Poland September 3–8, 2007 Fieldtrip Guide*.
- Szurliés, M., 2020.** Magnetostratigraphy of the Zechstein: Implications for the Late Permian geological time-scale. *Schriftenreihe der Deutschen Gesellschaft für Geowissenschaften*, **89**: 129–143.
- Tarkowski, R., Wdowin, M., 2011.** Petrophysical and mineralogical research on the Influence of CO₂ injection on Mesozoic reservoir and caprocks from the Polish Lowlands. *Oil and Gas Science and Technology – Rev. IFP Energies Nouvelles*, **66**: 137–150; <https://doi.org/10.2516/ogst/2011005>
- Tømmerås, A., Mann, U., 2008.** Improved hydrocarbon charge prediction by source-rock modeling. *Petroleum Geoscience*, **14**: 291–299; <https://doi.org/10.1144/1354-079308-766>

- Tyson, R.V., 2001.** Sedimentation rate, dilution, preservation and total organic carbon: some results of a modelling study. *Organic Geochemistry*, **32**: 333–339; [https://doi.org/10.1016/S0146-6380\(00\)00161-3](https://doi.org/10.1016/S0146-6380(00)00161-3)
- Tyson, R.V., 2005.** The "productivity versus preservation" controversy: cause, flaws, and resolution. *SEPM Special Publication*, **82**: 17–33.
- Toboła, T., Botor, D., 2020.** Raman spectroscopy of organic matter and rare minerals in the Kłodawa Salt Dome (Central Poland) cap-rock and Triassic cover - indicators of hydrothermal solution migration. *Spectrochimica Acta, Part A, Molecular and Biomolecular Spectroscopy*, **231**, 118121; <https://doi.org/10.1016/j.saa.2020.118121>
- Underhill, J.R., Richardson, N., 2022.** Geological controls on petroleum plays and future opportunities in the North Sea Rift Super Basin. *AAPG Bulletin*, **106**: 573–631; <https://doi.org/10.1306/07132120084>
- Van Wees, J.D., Stephenson, R.A., Ziegler, P.A., Bayer, U., McCann, T., Dadlez, R., Gaupp, R., Narkiewicz, M., Bitzer, F., Scheck, M., 2000.** On the origin of the Southern Permian Basin, Central Europe. *Marine and Petroleum Geology*, **17**: 43–59; [https://doi.org/10.1016/S0264-8172\(99\)00052-5](https://doi.org/10.1016/S0264-8172(99)00052-5)
- Vigran, J.O., Mørk, A., Forsberg, A.W., Weiss, H.M., Weitschat, W., 2008.** Tasmanites algae-contributors to the Middle Triassic hydrocarbon source rocks of Svalbard and the Barents shelf. *Polar Research*, **27**, 360–371; <https://doi.org/10.1111/j.1751-8369.2008.00084>
- von Eynatten, H., Kley, J., Dunkl, I., Hoffmann, V.E., Simon, A., 2021.** Late Cretaceous to Paleogene exhumation in central Europe – localized inversion vs. large-scale domal uplift. *Solid Earth*, **12**: 935–958; <https://doi.org/10.5194/se-12-935-2021>
- Wagner, M., 1999.** Vitrinite reflectance in selected boreholes from the Polish Basin (Polish Lowland). Unpublished report, AGH (in Polish).
- Wagner, R., 1994.** Stratigraphy and evolution of the Zechstein Basin in the Polish Lowland (in Polish with English summary). *Prace Państwowego Instytutu Geologicznego*, **146**: 1–71.
- Wagner, R., 2001.** Fauna i flora w basenie permskim (in Polish). In: *Budowa geologiczna Polski 3, Młodszy Paleozoik, Perm* (eds. M. Pajchłowa and R. Wagner): 16–18.
- Waples, D.W., 1980.** Time and temperature in petroleum formation: application of Lopatin's method to petroleum exploration. *AAPG Bulletin*, **64**: 916–926; <https://doi.org/10.1306/2F9193D2-16CE-11D7-8645000102C1865D>
- Waples, D., Kamata, H., Suizu, M., 1992.** The art of the maturity modeling - overview of methods. *AAPG Bulletin*, **76**: 31–46; <https://doi.org/10.1306/BDF875E-1718-11D7-8645000102C1865D>
- Wesenlund, F., Grundvåg, S.A., Sjøholt-Engelschiøn, V., Thießen, O., Pedersen, J.H., 2021.** Linking facies variations, organic carbon richness and bulk bitumen content – a case study of the organic-rich Middle Triassic shales from eastern Svalbard. *Marine and Petroleum Geology*, **132**: 105168; <https://doi.org/10.1016/j.marpetgeo.2021.105168>
- Więclaw, D., 2016.** Habitat and hydrocarbon potential of the Kimmeridgian strata in the central part of the Polish Lowlands. *Geological Quarterly*, **60** (1): 192–210; <https://doi.org/10.7306/gq.1260>
- Wilczek, T., 1986.** Assessment of the possibility of the hydrocarbon generation in the Mesozoic source rocks of Polish Basin (in Polish with English summary). *Przegląd Geologiczny*, **34**: 496–502.
- Wójcik, K., Zacharski, J., Łojek, M., Wróblewska, S., Kiersnowski, H., Waśkiewicz, K., Wójcicki, A., Laskowicz, R., Sobieñ, K., Peryt, T., Chylińska-Macios, A., Sienkiewicz, J., 2022.** New opportunities for oil and gas exploration in Poland-a review. *Energies*, **15**: 1739; <https://doi.org/10.3390/en15051739>
- Wygrala, B.P., 1989.** Integrated study of an oil field in the southern Po Basin, northern Italy. *Berichte der Kernforschungsanlage Jülich*, No 2313, Ph.D. Thesis, University of Cologne, Germany.
- Zakrzewski, A., Kosakowski, P., Waliczek, M., Kowalski, A., 2020.** Polycyclic aromatic hydrocarbons in Middle Jurassic sediments of the Polish Basin provide evidence for high-temperature palaeo-wildfires. *Organic Geochemistry*, **145**: 104037; <https://doi.org/10.1016/j.orggeochem.2020.104037>
- Zakrzewski, A., Waliczek, M., Kosakowski, P., Pańczak, J., 2022a.** Lower Jurassic in the central part of the Polish Basin - Geochemical and petrological approach, *Marine and Petroleum Geology*, **146**: 105922; <https://doi.org/10.1016/j.marpetgeo.2022.105922>
- Zakrzewski, A., Waliczek, M., Kosakowski, P., 2022b.** Geochemical and petrological characteristics of the Middle Jurassic organic-rich siliciclastic sediments from the central part of the Polish Basin. *International Journal of Coal Geology*, **255**: 103986; <https://doi.org/10.1016/j.coal.2022.103986>
- Ziegler, P.A., 1990a.** Collision related intra-plate compression deformations in Western and Central Europe. *Journal of Geodynamics*, **11**: 357–388; [https://doi.org/10.1016/0264-3707\(90\)90017-O](https://doi.org/10.1016/0264-3707(90)90017-O)
- Ziegler, P.A., 1990b.** *Geological Atlas of Western and Central Europe*. 2nd ed. Shell Internationale Petroleum Mij. BV and Geological Society of London.
- Zielinski, G.W., Poprawa, P., Szewczyk, J., Grotek, I., Kiersnowski, H., Zielinski, R.L.B., 2012.** Thermal effects of Zechstein salt and the Early to Middle Jurassic hydrothermal event in the central Polish Basin. *AAPG Bulletin*, **96**: 1981–1996; <https://doi.org/10.1306/04021211142>
- Żuk, T. (ed.), 2019.** Hydrocarbon prospective of Poland. Pyrzyce tender area. Fourth licensing round concessions for hydrocarbon prospecting, exploration and production in Poland (in Polish with English summary). *PIG Warszawa web data base*, access on 18 January 2022.